

**Investigating Variability in CO<sub>2</sub> Fluxes in Urban Gardens, Oakland CA**

A Thesis submitted to the faculty of  
San Francisco State University  
In partial fulfillment of  
the requirements for  
the Degree

Master of Arts

In

Geography

by

Patrick John Ehhalt

San Francisco, California

May 2022

Copyright by  
Patrick John Ehhalt  
2022

## **Certification of Approval**

I certify that I have read Investigating Variability in CO<sub>2</sub> Fluxes in Urban Gardens, Oakland CA by Patrick John Ehhalt, and that in my opinion this work meets the criteria for approving a thesis submitted in partial fulfillment of the requirement for the degree Master of Arts in Geography at San Francisco State University.

---

Andrew Oliphant, Ph.D.  
Professor,  
Thesis Committee Chair

---

Sara Baguskas, Ph.D.  
Associate Professor

## Investigating Variability in CO<sub>2</sub> Fluxes in Urban Gardens, Oakland CA

Patrick John Ehhalt  
San Francisco, California  
2022

One of the many strategies used to advance climate mitigation research involves investigating variability in biogenic CO<sub>2</sub> in the urban environment. A limited number of studies have focused on urban residential gardens and their contributions to the carbon cycle. This study used the closed chamber method to capture a snapshot in both time and space of the variability of CO<sub>2</sub> and H<sub>2</sub>O fluxes from two residential front gardens in Oakland Ca. The fluxes of CO<sub>2</sub> from two lawns, a common perennial grass, *Lomandra longifolia*, and decorative bark were measured to determine Net Ecosystem Exchange (NEE) of the various ground covers. Our results show that the NEE at both lawns proved to be strong carbon sinks, during peak photosynthesis, however differed significantly in magnitude. Meanwhile, our bark and *L. longifolia* samples proved to be small sources of CO<sub>2</sub> and similar in magnitude. Further, we were able to determine the Gross Primary Productivity (GPP) and ecosystem respiration (R<sub>eco</sub>) at each vegetated sample plot, where results show lawn plots, due to a much higher percentage of canopy cover, have a much greater GPP than *L. longifolia*. However, R<sub>eco</sub> from lawns measured approximately twice as much CO<sub>2</sub> than our *L. longifolia* or bark plots. Furthermore, we estimated the autotrophic respiration (R<sub>auto</sub>) from *L. longifolia*, where R<sub>auto</sub> rates were very small, likely due to *L. longifolia* only taking up a small portion of chamber footprint area. Observed GPP was further used to

estimate the carbon sequestration capacities of each type of vegetation by scaling up Fractional Green Canopy Cover (FGCC). Our estimates show that *L. longifolia*, at 100 percent FGCC had estimated carbon sequestration capacities similar to those of our lawn samples. Using this information, along with comparing the soil moisture and evapotranspiration rates between vegetated plots we determined *L. longifolia* to be a good plant choice for reducing CO<sub>2</sub> emissions gardens while using less water than required for lawns.

## **Acknowledgements**

I'd like to thank all of my fellow classmates and educators who have helped shape my adult academic career. Also, to my friends, who showed unwavering support in me going back to school. To my neighbors who graciously volunteered their gardens in the name of climate change research, this includes Shirley, who kept me well fed and hydrated — thanks. Two special thanks go out to Andrew Oliphant and Sara Baguskas for sharing their expertise and enthusiasm for micrometeorology which made this project especially interesting and fun. An enormous thank you to my partner Kelsey, whose inspiration and encouragement made this journey possible. Lastly, to Bridget and Maceo, my children, thank you. You kept me grounded.

## Table of Contents

<b>Certification of Approval</b> .....	<b>iii</b>
<b>Acknowledgements</b> .....	<b>vi</b>
<b>Table of Contents</b> .....	<b>vii</b>
<b>List of Tables</b> .....	<b>ix</b>
<b>List of Figures</b> .....	<b>x</b>
<b>List of Appendices</b> .....	<b>xii</b>
<b>1 Introduction</b> .....	<b>2</b>
<b>1.1 Background</b> .....	<b>2</b>
<b>1.2 The carbon cycle in an urban garden environment</b> .....	<b>2</b>
<b>1.3 Environmental drivers of carbon cycling associated with the urban setting</b> .....	<b>5</b>
<b>1.4 Carbon cycling in common urban ground covers</b> .....	<b>6</b>
1.4.1 Turf grass .....	6
1.4.2 Ornamental plants .....	8
1.4.3 Mulch .....	9
1.4.4 Compost .....	11
<b>1.5 Indirect emissions associated with urban gardens</b> .....	<b>13</b>
<b>1.6 CO<sub>2</sub> Flux Quantification</b> .....	<b>14</b>
<b>1.7 Research objective</b> .....	<b>15</b>
<b>2 Methods and Materials</b> .....	<b>17</b>
<b>2.1 Pilot study and Site selection</b> .....	<b>17</b>
<b>2.2 Study Area, Site history and climate</b> .....	<b>19</b>
<b>2.2 Chamber measurement principles</b> .....	<b>23</b>
<b>2.3 Chamber Design</b> .....	<b>24</b>
<b>2.4 Experimental Design</b> .....	<b>25</b>
<b>2.5 Data Processing</b> .....	<b>28</b>
<b>2.6 Data Analysis</b> .....	<b>28</b>
<b>3 Results</b> .....	<b>30</b>
<b>3.1 Soil characteristics and meteorological conditions throughout study</b> .....	<b>30</b>

<b>3.2 Chamber fluxes .....</b>	<b>34</b>
<b>3.2 Estimated GPP associated with various Fractional Green Canopy Cover .....</b>	<b>39</b>
<b>3.3 GPP of lawns and carbon sequestration potential of <i>L. longifolia</i> .....</b>	<b>40</b>
<b>3.4 Autotrophic Respiration from <i>L. longifolia</i>.....</b>	<b>41</b>
<b>3.5 Water Use .....</b>	<b>42</b>
<b>4 Discussion.....</b>	<b>44</b>
<b>5 Conclusion .....</b>	<b>46</b>
<b>6 References .....</b>	<b>48</b>

## List of Tables

Table 1. Carbon flux observations and estimations from turf grasses.....Error! Bookmark not defined.	
Table 2. Carbon flux observations and estimations from mulches.....	<b>11</b>
Table 3. Carbon flux observations and estimations from studies which included different applications of compost. ....Error! Bookmark not defined.	
Table 4. Average NEE, GPP and $R_{eco}$ values, in units of $mgCO_2 m^{-2} s^{-1}$ , for all vegetated plots over the entire study period.....	<b>39</b>
Table 5. FGCC observation measurements with $GPP_{100}$ estimations.....	<b>40</b>
Table 6. Evapotranspiration, soil moisture and $GPP_{obs}$ for all vegetated plots. Evapotranspiration based on the averages of $H_2O$ flux observations over the entire study. ....	<b>43</b>

## List of Figures

Figure 1. A conceptual model of the carbon cycle in the urban environment. (Source: modified image by Kimberley Navabpour).....	3
Figure 2. An example of the pilot study sampling method showing the chamber during observation. Pink flags indicate the remaining four sample plots along the lawn transect. ....	18
Figure 3. Study area information including (a) the regional setting of San Francisco Bay (b) a map of the study area, and (c) an image depicting a typical street found within the neighborhood/study area(c). (Source, image C: Google Maps) .....	19
Figure 4. An example of the darkened closed chamber connected to data logger and laptop used to measure ecosystem respiration on Lawn A. ....	21
Figure 5. An example of the transparent closed chamber connected to data logger and laptop used to measure CO <sub>2</sub> concentration in Lawn B. (Photo: Andrew Oliphant) .....	22
Figure 6. A side-by-side comparison between images of a juvenile and mature <i>L. longifolia</i> based on size. Left image shows our sample L3 next to a standard student ID card. A mature and much larger <i>L. longifolia</i> , noticeable by the relationship to the size of the stairs on the right side of the image. (Sources: Patrick Ehhalt (left), San Marcos Growers (right)).....	23
Figure 7. Side-by-side comparison of the difference between a digital color image of a lawn sample plot next to the same imaged processed using the Canopeo app.....	27
Figure 8. Plot average soil temperature per vegetated plot for each day we sampled across the entire study period.....	30
Figure 9. Box plot showing the variability in soil temperatures for vegetated plots over the entire study period.....	31
Figure 10. Plot average soil moisture observations for each vegetated plot with markers highlighting individual days of light precipitation recorded at the OAKLAND MUSEUM, CA US weather station (NOAA). ....	32
Figure 11. Box plot showing the variability in soil moisture across all vegetated plots for the entire study period.....	33

Figure 12. Box plot shows CO<sub>2</sub> fluxes of grouped *L. longifolia*, grouped bark plots and Lawns A and Lawn B, in ascending order based on each vegetated plot's flux mean ..... 35

Figure 13. Relationship between CO<sub>2</sub> flux and T<sub>soil</sub> including linear regression analysis for the three *L. longifolia* plots. .... 36

Figure 14. A linear regression shows the relationship between calculated plot average soil moisture and observed average R<sub>eco</sub> for both lawns over the entire study period. .... 36

Figure 15. Box plot showing R<sub>eco</sub> of all plots, in ascending order based on R<sub>eco</sub> means across the entire study..... 37

Figure 16. A linear regression shows the relationship between measured soil moisture and average GPP for both lawns over the entire study period..... 38

Figure 17. Estimated GPP<sub>100</sub> for all vegetated plots. Each lawn GPP<sub>100</sub> estimate shown further separated by observation periods 1 and 2 based on changes in FGCC. Observation 1 reflects observed GPP averages across the period from the start of study until our second FGCC observation (19 days). Observation 2 reflects the average GPP for the remainder of the study (8 days). Estimated GPP<sub>100</sub> from *L. longifolias* based on average observed GPP from entire study.41

Figure 18. Autotrophic respiration based on calculated averages for all *L. longifolia* over entire study period..... 42

## List of Appendices

Appendix A. One-way ANOVA test and Tukey HSD test results for $T_{\text{soil}}$ on all plots .....	55
Appendix B. One-way ANOVA test and Tukey HSD test results for $T_{\text{soil}}$ on all <i>L. longifolia</i> plots .....	56
Appendix C. One-way ANOVA test and Tukey HSD test results for soil moisture on all plots .	57
Appendix D. One-way ANOVA test and Tukey HSD test results for NEE on <i>L. longifolia</i> plots .....	58
Appendix E. One-way ANOVA test and Tukey HSD test results for NEE on bark plots .....	59
Appendix F. One-way ANOVA test and Tukey HSD test results for $R_{\text{eco}}$ on <i>L. longifolia</i> plots	60
Appendix G. One-way ANOVA test and Tukey HSD test results for GPP on <i>L. longifolia</i> plots	61

## **1 Introduction**

### **1.1 Background**

Earth has been experiencing an unprecedented increase in atmospheric carbon dioxide (CO<sub>2</sub>) concentration over the last 150 years (IPCC 2014). As a result, our planet has warmed by an average of approximately 1 °C in the last century (IPCC 2018). At the crux, is a combination of a steep increase in population and that population's reliance on the burning of fossil fuels for energy (The World Bank 2021). Fossil fuel based energy use is a growing concern in relation to urbanization, especially since 2007 marked the first time in history when more people were living in cities than in rural environments. This growth in population has potential to further increase CO<sub>2</sub> concentrations to an already large amount of Greenhouse Gas (GHG) emissions ascribed to urban areas. Therefore, there is a growing need to reduce GHG emissions from cities or to increase GHG sequestration through urban vegetation. In order to better understand the urban carbon cycle, climate mitigation research includes investigating the role of biogenic CO<sub>2</sub> fluxes in the urban areas (e.g. Velasco et al. 2013).

### **1.2 The carbon cycle in an urban garden environment**

Ecosystem respiration ( $R_{eco}$ ) is the combination of autotrophic ( $R_{auto}$ ) and heterotrophic respiration ( $R_{het}$ ).  $R_{het}$  and  $R_{auto}$  together, and/or individually, play instrumental roles in the carbon cycle as they both release CO<sub>2</sub> into the atmosphere (Figure 1).  $R_{auto}$  is a function of root and mycorrhizal activity below ground, and a function of released CO<sub>2</sub> and water vapor via stomata conductance aboveground.  $R_{het}$  is a function of the decomposition of vegetated debris and soil organic matter (SOM) which is broken down by microbes and enzymes (Ryan and Law

2005).  $R_{het}$  and  $R_{auto}$  are governed most strongly by soil temperature ( $T_{soil}$ ) and soil moisture (soil moisture) (Raich and Tufekcioglu 2000; Singh and Gupta 1977).  $R_{auto}$  and  $R_{het}$  are often anthropogenically controlled in the urban garden ecosystem due to changing substrate characteristics like soil temperature ( $T_{soil}$ ), soil moisture, soil pH, and soil bulk density as result of gardening maintenance (Velasco et al. 2021).

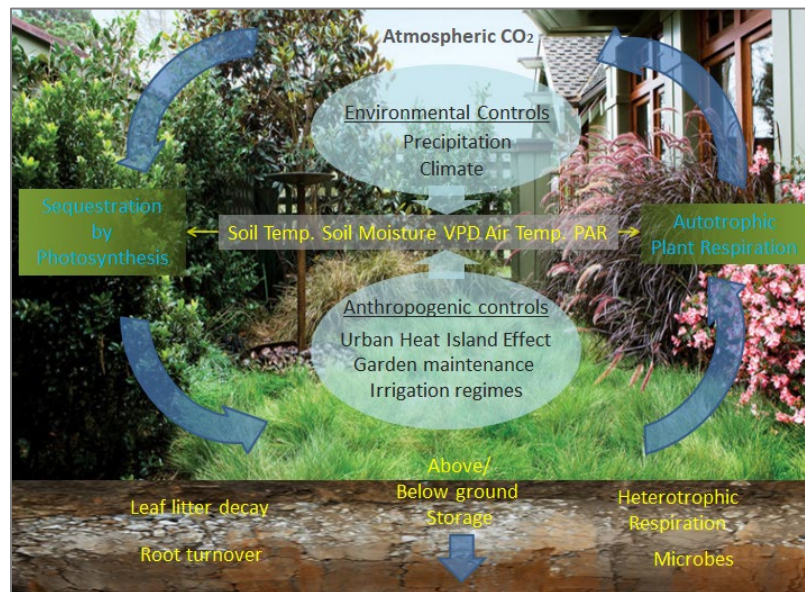


Figure 1. A conceptual model of the carbon cycle in the urban environment. (Source: modified image by Kimberley Navabpour)

Opposite to  $R_{eco}$  is photosynthesis, i.e., the uptake of  $CO_2$  by plants from the atmosphere. Plants rely on water availability,  $CO_2$ , and photosynthetic active radiation (PAR) to conduct photosynthesis. PAR is the portion of solar radiation that is absorbed by chlorophyll in leaves that drives photosynthesis. Stomatal opening (and closing) is also sensitive to changes in PAR, thus the absorption of  $CO_2$  (Churkina 2016). In an urban garden setting, decreased PAR through local shading due to the built environment and/or trees can affect photosynthesis. In addition,

high air pollution may decrease PAR. However, the aerosols in pollution can help offset diminished sequestration as aerosols scatter light, producing diffused PAR, and some plants/trees have shown a better photosynthetic response to diffused PAR opposed to direct beam PAR (Berry and Goldsmith 2020; Oliphant et al. 2011).  $T_{\text{air}}$  is generally positively correlated with photosynthesis, and may promote photosynthesis due to the Urban Heat Island effect (UHI); however exceeded  $T_{\text{air}}$  thresholds can lead to plant stress.

The Urban Heat Island effect (UHI) increases surface  $T_{\text{air}}$  and  $T_{\text{soil}}$  as a result of land use change associated with urbanization. UHI and the urban carbon cycle are coupled because UHI factors can control the rate of photosynthesis and  $R_{\text{eco}}$  (Vasenev et al. 2021). For example, increased  $T_{\text{soil}}$  from consequences associated to UHI (decrease nighttime cooling, trapped air, and waste heat from industry and transportation) can lead to higher evaporation rates resulting in drier soils which can exacerbate heterotrophic respiration ( $R_{\text{het}}$ ), particularly in dry climates or dry seasons if not irrigated (Kaye, McCulley, and Burke 2005). Also, sky view factor (SVF) is strongly modified by urban form. The SVF describes the ratio between the radiation measured at a point on Earth and that identical location unobstructed. SVF decreases surface cooling of gardens at night through reduced radiative loss (making frosts less frequent), and produces heterogeneous patterns of shading during the day.

Vapor pressure deficit (VPD) is the difference between atmospheric saturation vapor pressure and the actual water vapor pressure (Wherley and Sinclair 2009). High VPD causes plants to close their stomata to minimize water loss, decreasing photosynthesis (Grossiord et al. 2020). In addition, transpiration rates increase with elevated VPD, which adds to plant water stress. Further, high VPD has also shown to increase rates of water loss from moist soils, causing

drying and heating of the earth's surfaces, further exacerbating physiological dysfunction in plants (Dai 2013). Forced by recent rising global surface temperatures, the global increases to VPD percentages need to be considered in the urban garden carbon cycle.

### **1.3 Environmental drivers of carbon cycling associated with the urban setting**

$T_{\text{soil}}$  is a widely used variable when investigating the correlation between environmental conditions and  $\text{CO}_2$  fluxes from soil in urban micro-scale studies (Beesley 2012; Livesley et al. 2010; Shchepeleva et al. 2017).  $T_{\text{soil}}$  is a good predictor of  $\text{CO}_2$  fluxes from the soil because it controls microbial activity. However, 15 °C and 30 °C generally defines the temperature thresholds of microbial activity in most soils. Largely collected by *in situ* probing, urban micrometeorologists have used data to show highly positive correlations between  $T_{\text{soil}}$  and  $\text{CO}_2$  emissions (Bezyk et al. 2018; Hill et al. 2021). In addition,  $T_{\text{soil}}$  has statistically shown to be the most significant explanatory variable that controls  $R_{\text{het}}$  and/or  $R_{\text{auto}}$  rates (Goenster et al. 2015).

Similarly to  $T_{\text{soil}}$ , soil moisture is well represented in the literature for its effects on plant physiology and  $R_{\text{eco}}$  (Chadha et al. 2018). Soil moisture is controlled by irrigation application and/or precipitation and measured through a variety of methods (e.g. coring samples, depth of water table, soil probes, lab tests, gravimetric analysis). Soil moisture is important to plant growth, which can be measured by leaf area and size, which factor into  $R_{\text{auto}}$  and photosynthesis (Chadha et al. 2018; Ito 2020). Further, soil moisture is also a key control on  $R_{\text{auto}}$  by affecting respiration via root and leaf transpiration. Moreover, studies have shown that decreased soil moisture can have negative effects on fungicidal and microbial activity, as well as earthworm densities, bringing down  $R_{\text{het}}$  (Byrne, Bruns, and Kim 2008). Urban  $\text{CO}_2$  flux studies have shown

various degrees of significance of soil moisture to  $R_{\text{soil}}$ . For example Bezyk et al. (2018) showed high correlations ( $R^2=0.83$ ) between soil moisture and  $R_{\text{soil}}$ , while Livesley et al. (2010) and Shchepeleva et al. (2017a) deemed soil moisture insignificant. One explanation may be that their study sites had steady precipitation and consistently cool temperatures (Beesley 2012).

## **1.4 Carbon cycling in common urban ground covers**

Residential urban gardens can have a diverse array of plants and ground cover types. Often chosen for aesthetics, climate suitability and/or ecosystem services (recreation applications, carbon sequestration, status symbols), urban gardens are often some combination of ornamental plants, a variation of a turf grass, and mulch (Krekel, Kolbe, and Wüstemann 2016).

### **1.4.1 Turf grass**

Turf grasses make up 163,800 km<sup>2</sup> in the continental U.S.; roughly the size of California (and three times larger than that of any irrigated crop) (Milesi et al. 2005). Turf grasses are often the primary vegetated land cover in urban environments (Kaye, McCulley, and Burke 2005). Not to be confused with grassland studies (which are also well represented in the literature), urban turf grasses are frequently an area of focus for researchers who employ the EC and chamber methods (Velasco et al. 2021). Found in public greenspaces, business parks, sports fields and private residences, turf grasses are a popular choice of land use for their ecosystem services: aesthetics, recreation applications, carbon sequestration, status symbols, and more (Krekel, Kolbe, and Wüstemann 2016; White et al. 2013; Monteiro 2017). To maximize ecosystem services, urban turf grasses are maintained, using a wide range of management practices. Although limited, there are micrometeorological projects that compare CO<sub>2</sub> fluxes based on different combinations of irrigation, mowing regimes and soil amendments (Livesley et al. 2010;

Shchepeleva et al. 2017; Velasco et al. 2021). For example, Velasco et al. (2021) measured soil CO<sub>2</sub> efflux, CO<sub>2</sub> production, and CO<sub>2</sub> storage in a residential lawn of Singapore for close to three years. Their study also included emissions from fossil fuel consumption associated with mowing equipment (Velasco et al. 2021). They concluded that by limiting mowing to once every three weeks and not incinerating grass clippings, their turf study area could serve as a carbon sink. Moreover, CO<sub>2</sub> flux rates of turf grass have been used in comparisons to other common urban land covers, such as bark and, vegetated ground covers and shrubs. In addition, turf research has included the comparison of forest floors and agricultural fields to urban environments to investigate how disrupted soils, under different management and irrigation strategies, affected CO<sub>2</sub> fluxes (Table 1) (Chun et al. 2014; Kaye, McCulley, and Burke 2005).

Table 1. Carbon flux observations and estimations from turf grasses

Author	Location	Role of turf grass in study	Max. Turf grass Flux (gCm <sup>-2</sup> y <sup>-1</sup> ) <sup>*</sup>
Hill et al. 2021	Baltimore, Maryland US	Turf fluxes were compared to fluxes from a neighboring forest floor over 4 years to examine daily, seasonal and annual patterns of biogenic CO <sub>2</sub> emissions	1220±31 <sub>F</sub>
Kaye et al. 2005	Fort Collins, Colorado US	Well-maintained urban lawns paired against nearby native shortgrass steppe, dryland wheat-fallow and irrigated corn	2394±284 <sub>a</sub>
Livesley et al. 2010	Melbourne, Victoria AUS	Lawn systems, under various water and fertilizer regimes were evaluated alongside undisturbed and mulched garden beds	3942 <sub>b</sub>
Shchepeleva et al. 2017	Moscow RU	Organic layer depths of 5,10 & 20 cm below turf grass studied to determine diminishing CO <sub>2</sub> emissions over a 3 year period	1472 ± 52 <sub>F</sub>
Townsend-Small et al. 2009	Irvine, California US	Comparison of ornamental to athletic turf based on a scenario including fuel consumption, fertilization, and irrigation, in addition to measured turf fluxes as part of the estimation of the net GWP <sub>1</sub>	285 <sub>c,d,F</sub>
			798 <sub>c,e,F</sub>

<sup>\*</sup> Positive numbers represent a carbon source  
<sup>a</sup> Allometry and soil gas chamber used to estimate above ground NPP, <sup>b</sup> C sequestration gauged based on a synthesis found in (Soussana et al. 2007),  
<sup>c</sup> CO<sub>2</sub> equivalent based on measured N<sub>2</sub>O  
<sup>d</sup> ornamental lawn, <sup>e</sup> athletic field  
<sup>F</sup> based on NEE  
<sup>1</sup> GWP – Global warming potential

By and large, turf grass ecosystems in urban environments are reported to be sources of CO<sub>2</sub>, when considering the full annual cycle. Moreover, when including indirect emissions, e.g. mowing equipment, total emissions associated with turf grasses increase. However indirect emissions are understudied. Based on the wide search of the literature surrounding CO<sub>2</sub> fluxes on turf, the majority of studies reported turf/lawn as strong sources of carbon (thousands of gC m<sup>-2</sup> y<sup>-1</sup>). A limited number of chamber-based studies revealed only trace net emissions of CO<sub>2</sub>, and even fewer reported turf as carbon sinks (Table 1). However, a limited amount of studies include the carbon sequestration rates of turf through photosynthesis, and only measure respiration, thus leaving even fewer studies with complete NEE estimates. Then again, Velasco et al. (2021) and Townsend-Small and Czimczik (2010) concluded that turf grasses could serve as sinks under a “conservative” maintenance strategy. “Conservative” strategies include reducing the application of inorganic fertilizers, diminishing irrigation, and removing fuel consumption associated with mowing and leaf blowing. Only then can urban turf grass mitigate greenhouse gas emissions in cities (Townsend-Small and Czimczik 2010).

#### **1.4.2 Ornamental plants**

Ornamental plants used in residential-scale urban landscapes have many documented benefits, however the literature investigating their potential for carbon sequestration is limited (Whittinghill et al. 2014). Extensive research in plant physiology may aid researchers in estimating sequestration rates per species. However because photosynthesis is determined by many *in situ* conditions simply basing sequestration rates on physiological characteristics could limit designing residential gardens based on sequestration capacities specific to a certain species

(Korsakova, Plugatar, and Ilnitsky 2019). In addition, instantaneous leaf-level measurements of photosynthesis do not tell us how much carbon is sequestered over longer periods of time.

In two studies which investigate sequestration potentials in ornamental plants, neither include a flux chamber. Instead, Whittinghill et al. (2014) studied the sequestration potential of shrubs and groundcovers in an urban setting by measuring soil carbon gains over a two year period. General conclusions were that the woody plants, herbaceous perennials and native grasses sequestered the most carbon. Wang, Chang, and Li (2021) built computer-based models to estimate photosynthesis by using remote sensing and field surveys to calculate leaf area which they then used with the chemical principle of photosynthesis (1 mol CO<sub>2</sub> absorbed, by the per unit leaf area of the plant, will result in 12 g carbon sequestered). Results suggest that out of the 19 species of commonly found shrubs in urban parks across Beijing, *Lagerstroemia indica* had the highest rate of at 3.16 gC m<sup>-2</sup> d<sup>-1</sup>. Moreover, the mean primary productivity of all 19 shrubs was 1.81 gC m<sup>-2</sup> d<sup>-1</sup>. These results contributed to the building of a framework that promotes designing urban parks with a focus on carbon sequestration.

### **1.4.3 Mulch**

Mulch is a layer of organic or inorganic material that separates the soils surface from the atmosphere (Pramanik et al. 2015). In urban gardens, organic mulch (wood chips or shredded bark) is often used for its garden aesthetics and ability to improve plant health by retaining moisture, regulating soil temperature and enriching soil (i.e. microbial activity, nutrition enhancement). These functions have shown to correlate strongly to carbon fluxes (Legiandenyi 2010). In some cases rocks or gravel is used as mulch. These inorganic mulches can have varying effects on plant health, like the dangers of extreme heat or cooling through albedo. Sheet

plastics and geotextile fabrics are forms of mulches used for weed suppression and reducing soil evaporative losses, but provide little nutritional benefit, nonetheless are still common in urban gardens. The study of the effect of rocks and sheet mulches on the carbon cycle in an urban garden is very limited.

Much like chamber studies involving urban turf grass, the quantification of CO<sub>2</sub> fluxes from mulched areas is limited (Haciogullari 2012; Legiandenyi 2010). However, because urban gardens often include mulched areas in close proximity to turfed areas, a few studies have been able to capture data from both types of land cover within the same study. For instance, Hundertmark et al. (2021) concluded that soil respiration from mulch was significantly higher, per unit area than in an adjacent lawn (Table 2). Similarly in method, Byrne, Bruns, and Kim (2008) were able to compare lawn, un-mowed grass, bark and gravel. Their conclusions showed that bark mulch averaged slightly lower in positive CO<sub>2</sub> fluxes than lawn over the entire study period (May-Aug). Yet, in July, CO<sub>2</sub> fluxes in the bark mulch exceeded all the other plots before diminishing significantly.

Table 2. Carbon flux observations and estimations from mulches

Author	Location	Role of mulch in study	Max. Mulch Flux ( $\mu\text{molCm}^{-2}\text{s}^{-1}$ )
Livesley et al. 2010	Melbourne, Victoria AUS	Lawn systems, under various water and fertilizer regimes were evaluated alongside undisturbed and mulched garden beds	0.138
Legiandenyi 2010	Baton Rouge, Louisiana US	Soil CO <sub>2</sub> fluxes from seven mulch types to investigate carbon dynamics of intensely managed urban forest ecosystems	21±0.5
			Max. Mulch Flux ( $\mu\text{molCO}_2\text{m}^{-2}\text{s}^{-1}$ )
Byrne, Bruns, and Kim 2008	Centre County, Pennsylvania US	Compare ecosystem properties based on residential landscape covers: lawns, bark mulch, gravel mulch and an un-mowed vegetation as a reference	8.6 <sup>-5</sup>
Mu, Fang, and Liang 2016	Yangling, Shaanxi CN	Plastic film mulch, plastic film with wheat straw, only wheat straw, and bare soil were analyzed for temporal and spatial variations of soil respiration in a greenhouse	7.2
Hundertmark et al. 2021	Boston, Massachusetts US	CO <sub>2</sub> fluxes from mulch and lawn, factoring C uptake by trees and grass, as well as anthropogenic CO <sub>2</sub> emissions associated with energy use of a university campus	8.5
Shahzad et al. 2019	Puyallup, Washington US	Soil-compost mix filled mesocosms covered with wood chips, cardboard mulch, landscape fabric, polyethylene film and a control to measure gas exchanges	3.6

#### 1.4.4 Compost

Of the few studies which have investigated the effects of compost on CO<sub>2</sub> emissions study objectives predominantly revolve around the role of compost in terms of health improvement for plant productivity, quantifying carbon storage, and carbon to nitrogen ratios; not in CO<sub>2</sub> flux calculations (Andersen et al. 2010; Memoli et al. 2017). Moreover, compost studies come by way of the agricultural and commercial compost industry. These studies consist of very diverse set of study objectives (Table 3). Therefore, experimental designs and units of measure for fluxes differ.

Table 3. Carbon flux observations and estimations from studies which included different applications of compost.

Author	Location	Role of compost in study	Max. emissions from study plot
Andersen et al. 2010	Kongens Lyngby, DEN	CO <sub>2</sub> ,CH <sub>4</sub> ,N <sub>2</sub> O emissions from 6 plots over 600days from the composting of organic household waste based on variety of mixing schedules and additions of compost	12.0 (gCh <sup>-1</sup> ) <sub>a</sub>
Beesley 2012	Liverpool UK	Soil respiration from a 35 year old urban lawn soil amended with different volumes of green waste compost compared to 2 newly created urban soils	3000 (gCm <sup>-2</sup> y <sup>-1</sup> ) <sub>b</sub>
Memoli et al. 2017	Napoli ITA	Comparison of 1 & 10 year effects of a single application of compost with a focus on microbial biomass and activity.	14.4 (gCO <sub>2</sub> <sup>-1</sup> d.w.10d <sup>-1</sup> ) <sub>c</sub>
SJV Air Pollution Control District 2013	San Juaquin Valley California, US	CO <sub>2</sub> emission results over a 30-day study which tested technological advancements applied to large composting facility	14227 (mgCO <sub>2</sub> m <sup>2</sup> min <sup>-1</sup> )
Vergara and Silver 2019	Nicasio, California US	Combination of methods used to continuously (91days) measure CO <sub>2</sub> ,CH <sub>4</sub> ,N <sub>2</sub> O emissions from full composting green waste and manure in a composting facility	3.0 (mgCO <sub>2</sub> m <sup>-2</sup> ) <sub>a</sub>

<sub>a</sub> flux based on varying volumes of air inside the unit (initially 0.32 m<sup>3</sup>) <sub>b</sub> at 45% compost. <sub>c</sub> "d.w."= 1gram soil

For instance, a waste management division of municipalities in central California investigated CO<sub>2</sub> emissions in an effort to become more sustainable (San Joaquin Valley Air Pollution Control District 2013; Vergara and Silver 2019). Studies like these can help fill the gap regarding compost emissions, as compost is a commonly used residential garden amendment.

Soil amendments, both chemical (artificial fertilizers) and natural (compost) are key components to plant productivity for their nutritional supplements, much of the reason why they are found in urban gardens. Compost is beneficial to plant growth and as a result can equate to more photosynthesis. A multitude of laboratory and field studies of wide-ranging temporal and spatial resolutions support that there are generally positive correlations between compost and microbial/enzymatic activity (Memoli et al. 2017; Ros et al. 2006; Saviozzi et al. 2006).

Therefore, it can be inferred that increased rates in the decomposition of SOM in compost also increases rates of  $R_{\text{het}}$  and  $R_{\text{auto}}$ . However, compost is also beneficial to plant growth and as a result can equate to more photosynthesis, justifying the need for studies which include both GPP and  $R_{\text{eco}}$ .

In a garden-scale  $\text{CO}_2$  mulch study Beesley (2012) used flux measurements from fieldwork, and sample in a lab, to determine the ranges of respiration between new and old urban soils which were amended with different concentrations of compost (15, 30, and 45 % by volume). Results showed significant increases of  $R_{\text{het}}$  under all conditions, in addition to increased  $T_{\text{soil}}$ . In terms of emissions, the difference between the means of the samples (at  $15^\circ\text{C}$ ) containing 0% compost versus 45% was approximately  $1800 \text{ gC m}^{-2} \text{ y}^{-1}$ .

While there is some understanding of the direct emissions of purchased compost, its indirect emissions are severely understudied. The transportation (commercial or private), and manufacturing of compost may offset carbon sequestration as a result of plant productivity (increased leaf area and biomass) however, these trade-offs have not been investigated in urban  $\text{CO}_2$  flux studies.

### **1.5 Indirect emissions associated with urban gardens**

Home garden maintenance often involves the emissions of  $\text{CO}_2$ , therefore can be associated with the urban carbon cycle. Few studies include the analysis of  $\text{CO}_2$  emissions associated with garden maintenance, like the manufacturing and transportation of landscaping trade tools, and soil amendments (Velasco et al. 2021). Internal combustion engines (ICE) are regularly found in common maintenance tools, like lawnmowers, trimmers and leaf blowers, where the combustion of carbon in the fuel produces exhaust that creates  $\text{CO}_2$  emissions.

Because of this, in some metropolitan areas, ICEs are prohibited for use in landscape maintenance (Saidani and Kim 2021). Townsend-Small and Czimeczik (2010) incorporated the “carbon cost” of maintenance by calculating the emissions from energy associated with pumping irrigation, fertilizer production, and fuel cost and consumption. Partial results revealed an additional  $122 \text{ gCO}_2 \text{ m}^{-2} \text{ yr}^{-1}$  in fuel usage alone (Townsend-Small and Czimeczik 2010b). Similarly, mowing (based on the frequency of every 2nd week) has shown to emit  $41.3 \text{ Mg CO}_2 \text{ km}^{-2} \text{ yr}^{-1}$  (Velasco et al. 2021). Moreover, electric gardening tools use energy which is generated in part by the burning of fossil fuels. While few studies directly incorporate the emissions of garden maintenance tools into residential garden GHG research, there is a vast and robust collection of literature focused on the carbon emissions and environmental impact of small ICEs (Saidani and Kim 2021).

### **1.6 CO<sub>2</sub> Flux Quantification**

The two methods most commonly used for measuring the exchange of CO<sub>2</sub> between land and atmosphere are the eddy covariance method (EC) and the closed-chamber (CC) method. Although developed largely for use in large-scale natural environments the EC method has afforded researchers the ability to quantify CO<sub>2</sub> fluxes in and around cities. The peer-reviewed literature which focuses on CO<sub>2</sub> fluxes using the EC method in urban environments, at the neighborhood-wide scale, is plentiful, however studies of narrower spatial scales are limited (Dyukarev 2017; Weissert, Salmond, and Schwendenmann 2014). The EC method isn't able to capture the individual contributions of different facets of the urban landscape easily due to the large heterogeneity in sources of GHGs within the measurement footprint. Moreover, the EC method is better suited for use at the neighborhood scale and larger, as teasing out biogenic

sources from anthropogenic sources is difficult and costly, leaving the CC method better suited for investigating variability in CO<sub>2</sub> fluxes at the garden-scale. However, the EC method can serve as a complimentary tool to the CC method as EC can measure continuously while chamber measurements can tease apart the spatial variability of carbon sources and sinks defined by different land cover types and their contribution to overall carbon fluxes within the footprint.

The net ecosystem exchange of CO<sub>2</sub> (NEE) with the atmosphere above is governed by two opposing (in direction) CO<sub>2</sub> fluxes from ecosystem respiration ( $R_{eco}$ ) and gross primary productivity (GPP), such that

$$NEE = GPP - R_{eco} , (1)$$

NEE, therefore represents the exchange rate of CO<sub>2</sub> over time and space, thus defining an ecosystem by their commonly used descriptive terms “sink” or “source”. In this study, the net sink of CO<sub>2</sub> over a period of time (atmosphere-ecosystem flux) is represented by a negative NEE value, while a net source produces a positive value.

### 1.7 Research objective

The goal of this study was to investigate how CO<sub>2</sub> fluxes varied across different ground cover types under a variety of environmental conditions in urban residential gardens. Our specific objectives were to:

1) Compare and contrast the CO<sub>2</sub> fluxes between the following ground cover types: California’s most common turf grass; Tall fescue, *Festuca arundinacea*; Fir-bark mulched areas; and a drought tolerant flowering grass, *L. longifolia* using the closed-chamber method.

2) Compare and contrast the carbon sequestration capacities between *L. longifolia* and two lawn turfs in early spring.

There are few CC studies involving urban residential gardens and more observational garden studies for a wide range of hydroclimates need to be generated, particularly those that compare common garden types for the region. Our study helps fill that research gap, even though our study only captured a snapshot, of both time and space, it provides a direct comparison of CO<sub>2</sub> fluxes between commonly selected garden cover types in the region. The closed chamber method has shown to be particularly useful in comparing different garden types in close proximity. By advancing research and improving our understanding of the carbon cycle at the garden-scale we can plan for the practices that produce the most ecosystem services with the lowest CO<sub>2</sub> emissions. This information can be used to produce best-practices for homeowners, city planners, and policy makers alike.

## 2 Methods and Materials

### 2.1 Pilot study and Site selection

Between the end of January and early February of 2022 we performed a pilot study to determine which specific gardens to use, what common ornamental plants were available and an appropriate size for sampling. The search parameters for finding suitable locations involved a) being close enough to one another (because we were on foot) where we conduct our chief study within an hour, on either side of solar noon and b) where plant density was sparse enough so our that our equipment did not affect the aesthesis/health of a volunteered garden. In total we sampled eight different plants and 3 different bark varietals, across six gardens. We decided to focus on two gardens within 50 m of each other that were similar lawns in terms of species and both in good health. In addition, one garden also had an area sparsely planted with drought tolerant plants (i.e. *Achillea millefolium*, *Eschscholzia californica*, *L. longifolia*).

One portion of our pilot study was used to determine how fluxes varied within a lawn and to estimate the number of samples appropriate to represent the lawn entirely. After narrowing down our search to two lawns we sampled 5 plots per lawn (in succession) along transects. Transect direction was determined by the need for each plot to be located in full sun (Figure 2). A T-test revealed there was not enough was evidence to accept the null hypothesis that the CO<sub>2</sub> fluxes within each lawn sample plot lawn were all equal (T-test,  $p=0.01$ ,  $\alpha=.05$ ).



Figure 2. An example of the pilot study sampling method showing the chamber during observation. Pink flags indicate the remaining four sample plots along the lawn transect.

As a result we chose to sample each lawn once per day in the one of the locations previously found along the pilot study transect, and where our equipment would remain on the sidewalk.

We also measured for soil moisture and  $T_{\text{soil}}$  directly following flux measurements. Along the same transects, we took one measurement in the approximate center of the chamber footprint. Results from a T-test revealed that that differences in soil moisture were statistically significant ( $p=0.006$ ,  $\alpha=.05$ ). Therefore, the decision was made to take four soil moisture samples per plot for all our sample plots in our chief study and use the average when calculating our results.

On the contrary, the differences in  $T_{\text{soil}}$  were small enough to be considered equal. However, because our instrument measured  $T_{\text{soil}}$  and soil moisture simultaneously, we chose to base  $T_{\text{soil}}$  results on the average of four measurements per plot as well.

## 2.2 Study Area, Site history and climate

Our study was conducted in the Piedmont Avenue neighborhood of Oakland, California. Much like the rest of the neighborhood, the street in which our sample gardens were located, the majority of homes are single family detached dwellings on properties averaging approximately 500 m<sup>2</sup>, with outdoor space typically given to lawns, trees, mulched and/or ornamental planted areas.

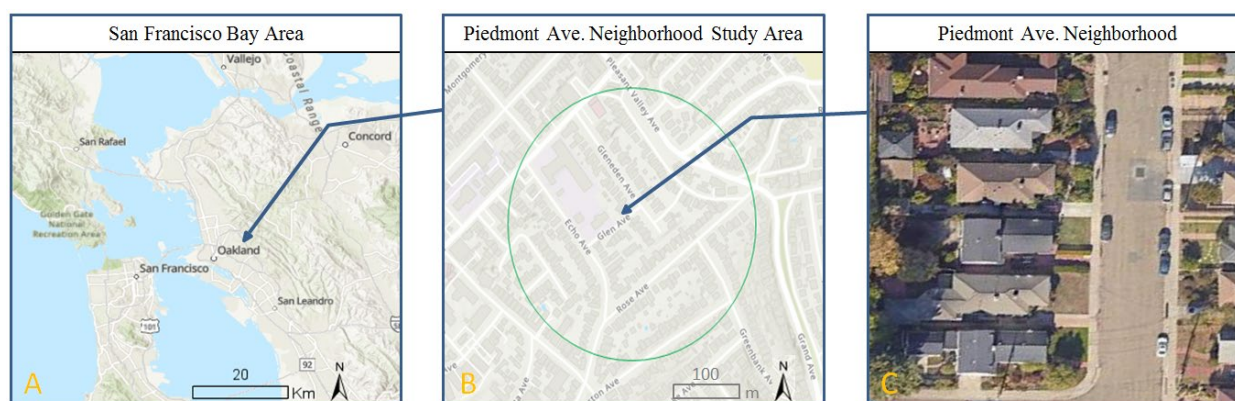


Figure 3. Study area information including (a) the regional setting of San Francisco Bay (b) a map of the study area, and (c) an image depicting a typical street found within the neighborhood/study area(c). (Source, image C: Google Maps)

Oakland Ca. has a Mediterranean climate (Köppen Csb): warm, dry summers, and mild, wet winters (NOAA). Based on long-term data (1991-2020), collected from the National Oceanic and Atmospheric Administration's Oakland Museum station (4 km away from the study site) shows that Oakland averages 260 sunny days and 663 mm of rain per year (NOAA). The five month portion (Oct. 2021 thru Feb.2022) of water year 2022 leading up to our experiment saw rainfall totals of 531.4 mm with a monthly maximum of 226.8 mm in Dec. 2021 and a monthly min of 0.5 mm in Feb. 2022 (NOAA). Our study site can also experience overcast low level

stratus, but not actually in contact with the ground and dripping. This type of advection fog typically burns off by late morning.

When originally inhabited by the native Ohlone people, this area supported an oak woodland habitat. Starting in the 1850's land use changed as urbanization began. Between the 1850's and 1939 our study sites would have been located on the estate grounds of the local landowner, where their aesthetic gardens fractured the homogeneity of the oak woodland (Wurm 1990). By 1940 the land was sold, a new road was put in, and lined with single family homes, which are still present today (Figure 3c) (Wurm 1990).

According to USDA-National Cooperatives Soil Survey (NCSS) the study site is categorized as NCSS soil 149—Urban land-Danville complex which has a typical horizon profile of clay loam 0 to 53 cm, sandy clay to 134 cm and silty clay loam to 203 cm, with a geomorphic position of an alluvial fan/footslope (USDA-NRCS, n.d.).

Our study area consisted primarily of single family homes set back from the street by 12 meters in which the space is typically occupied by a front garden. The two front gardens in which sampling took place, fell within a radius of approximately 160 meters from focus point 122.247N 37.829W (Figure 2b). The exact locations are not given to maintain the privacy for the homeowners who graciously gave permission for us to use their front gardens. Within that radius the large majority of gardens consisted of ornamental lawns, which varied greatly in lawn health, and/or drought tolerant landscaping (vegetative ground covers, woody perennials, shrubs, and mulch). Few gardens had small trees (<3m), and even fewer gardens had large trees (>3m).

Our total number of sample plots, per day, (n=13) were divided across two front gardens. Garden 1 provided a 20 m<sup>2</sup> lawn which we used for collecting Lawn A samples. Garden 1 also

provided an adjacent garden which was mulched with “micro” (0.6 cm) Fir bark and planted with a mix of California native shrubs and perennial drought tolerant grasses. Three of the grasses were *L. longifolia*, commonly known as Variegated Dwarf Mat Rush; a yellowish green, grass-like perennial bush often used locally in drought tolerant landscaping (Grampp 2022). Garden 2 was planted with approximately 20 m<sup>2</sup> of lawn, and was used to collect Lawn B samples. Lawn B was divided by a walkway.



Figure 4. An example of the darkened closed chamber connected to data logger and laptop used to measure ecosystem respiration on Lawn A.

At the beginning of our study, both lawns were in overall good health (verdant, few to zero dead patches with limited weeds) (Figures 4 and 5). Lawn A had its irrigation system shut off and was only getting water via precipitation whereas lawn B was void of an irrigation system. However, Lawn B was consistently wet, most likely due Glen Echo creek’s close proximity to the lawn. Maintenance regimes on our lawns differed slightly. Lawn A was on a mowing

scheduled of twice per month, while lawn “B” was mowed once a month. Neither lawn was amended with supplemental nutrients during our study.



Figure 5. An example of the transparent closed chamber connected to data logger and laptop used to measure CO<sub>2</sub> concentration in Lawn B. (Photo: Andrew Oliphant)

*L. longifolia* is an Australian native, drought tolerant perennial, rhizomatous herb with light yellowish-green, shiny, firm, and flat and narrow (8-12mm) leaves (Figure 6) (Ko 2015). They can grow up to 1m wide and 1m high. However, our three study specimens (L1, L2, L3) were newly planted (Jan. 2022) juveniles. Their leaves were sparse, and measured roughly 0.7 cm wide and no longer than 30cm. They were planted within in a grid of drip irrigation (1.5 cm tubing with 2 L/hour emitters every 30 cm) which was buried under 10 cm fir bark mulch. In addition, each *L. longifolia* received another short length (>10 cm) of irrigation tubing, connected to the grid, that had two more 2 L/hour emitters on it.



Figure 6. A side-by-side comparison between images of a juvenile and mature *L. longifolia* based on size. Left image shows our sample L3 next to a standard student ID card. A mature and much larger *L. longifolia*, noticeable by the relationship to the size of the stairs on the right side of the image. (Sources: Patrick Ehhalt (left), San Marcos Growers (right))

## 2.2 Chamber measurement principles

The concept behind our chamber method was to measure changes in concentration of CO<sub>2</sub> within the chamber over the period of about two minutes. Based on the rate of change, the chamber volume (V) and the area of surface footprint being measured (A) we calculated the net ecosystem-atmosphere flux (F) of CO<sub>2</sub> (Eq. 1). Our chamber measured 75 cm wide by 75 cm long by 75 cm high. CO<sub>2</sub> fluxes were calculated by multiplying the change in CO<sub>2</sub> ( $\Delta C$ ) (mgCO<sub>2</sub> m<sup>-2</sup>s<sup>-1</sup>), by the volume of the chamber (0.42 m<sup>3</sup>), divided by the area of the chamber (0.48 m<sup>2</sup>) (Equation1). Based on this concept the following equation was used to calculate the fluxes:

$$F = \Delta C \times \frac{V}{A}, (1)$$

NEE represents the exchange rate between the surface and atmosphere of CO<sub>2</sub> over time and space, thus defining an ecosystem by their commonly used descriptive terms “sink” or “source”.

However, NEE is the difference between ecosystem respiration ( $R_{eco}$ ) and Gross Primary Productivity (GPP). The following equation was used to calculate NEE:

$$NEE = GPP - R_{eco} , (2)$$

While NEE calculations were achieved using a transparent chamber we also used a dark chamber to isolate  $R_{eco}$ . A black, 3 mil thick, plastic sleeve was pulled over the transparent chamber to block out PAR, thus eliminating photosynthesis. This was done over all of our vegetated samples. By residuals we were able to calculate GPP (Eq. 3). GPP is the amount of CO<sub>2</sub> sequestered during photosynthesis by all producers within an ecosystem; in our case *L. longifolia* and lawn.

$$GPP = NEE - R_{eco} , (3)$$

The darkened chamber results were further used in combination with the flux results from transparent sampling to partition  $R_{eco}$  into heterotrophic ( $R_{het}$ ) and autotrophic respiration ( $R_{auto}$ ), however only for *L. longifolia*. Using the transparent chamber, we sampled all-bark plots as close to each *L. longifolia* as possible, without including *L. longifolia*. By doing so we attempted to mimic the *L. longifolia* sample plot without the plant present, offering estimated  $R_{het}$ . Using the following equation we calculated, through residuals,  $R_{auto}$  of each *L. longifolia* (Equation 3).

$$R_{eco} = R_{auto} + R_{het} , (4)$$

### 2.3 Chamber Design

The 0.42 m<sup>3</sup> chamber was constructed from white ¾ inch PVC pipe, and covered with Tefzel, a transparent plastic film designed to omit near infrared and UV light. Tefzel also has low

permeability to liquids, gases, moisture, and organic vapors. The chamber housed a non-dispersive, open path infrared gas analyzer (IRGA) (LI-7500, LiCor Inc. Lincoln, Nebraska) in addition to a quantum sensor which measures photosynthetically active radiation (PAR) in the waveband 0.4-0.7  $\mu\text{m}$  (LI-7500, LiCor Inc. Lincoln, Nebraska). A 4-inch 12VDC plastic fan runs continuously within the chamber to ensure sufficient mixing of air for representative gas concentration measurements. Two T-type thermocouples were used to measure ambient air temperature inside and outside the chamber. Instruments were connected to a data logger (CR 1000), while interfaced with a laptop, all powered by a 12-volt Super Start Marine Deep Cycle battery. All equipment was transported using an aluminum gardening cart.

## 2.4 Experimental Design

Sampling occurred every weekday between March 3rd and March 29th 2022 (except day 10) for a total of 18 sampling days. Every effort was made to keep the order of sample sites consistent, in addition to repeating the precise placement of the chamber. However, chamber placement varied slightly due to the impracticality of leaving permanent markers (for future reference) in a volunteered residential garden; chamber placement varied at most by 15 cm in any direction. We sampled three *L. longifolia* with the transparent chamber in addition to the same three using the dark chamber, plus three bark samples and Lawn A in one location and just Lawn B at another. The location of sample plots within each lawn site was selected to minimize foot traffic on the plots, as compaction has shown to alter respiration. In an effort to capture peak solar irradiance, and maximize photosynthetic activity of the study plants, sampling took place between 11:30am and 1:30pm Pacific Standard Time.

The deployment of the closed chamber involved placing the chamber over each individual sample plot (n=13) followed by sealing the chamber. Sealing consisted of wrapping a 3 meter long, 3/4 inch thick, and 1 Kg weldless chain against the outer bottom edge of the PVC chamber frame in an effort to create as much contact between the ground and the sheet-plastic flaps, which extended 6 inches away from the chamber. Creating the seal helped minimize perturbations to CO<sub>2</sub> concentration measurements caused by wind. While every effort was made to seal the chamber from ambient atmospheric conditions the potential for wind to influence CO<sub>2</sub> concentrations slightly was always a factor. All potential disturbances (wind gusts, shading) were documented in our field notes. Once sealed, a start time was recorded, and the chamber was left undisturbed for 120 seconds, after which it was moved to another sample site.

Soil temperature ( $T_{\text{soil}}$ ) and soil moisture (soil moisture) have shown to correlate highly to respiration (Chadha et al. 2018; Goenster et al. 2015). Environmental controls of  $T_{\text{soil}}$  and soil moisture include precipitation and climate in all ecosystems, however in urban garden environments anthropogenic driven factors such as UHI, irrigation and maintenance regimes can influence  $T_{\text{soil}}$  and soil moisture further. We measured  $T_{\text{soil}}$  and soil moisture using a Field Scout TDR 150 soil moisture meter. Soil moisture data was measured as volumetric water content (VWC). Each sample plot was probed at a depth of 9.5 cm in four locations within the footprint of the chamber measurements.

To make comparisons of the carbon sequestration capabilities between *L. longifolia* and lawns A and B, the observed GPP, in relation to its Fractional Green Canopy Cover (FGCC), was normalized to 100%. FGCC was calculated by the open-source, iPhone app, Canopeo. Canopeo is an image analysis tool that analyzes and classifies the ratios of Red/Green and

Blue/Green colors to produce a black and white image where white pixels correspond to the green canopy cover and black pixels which correspond to the pixels that are not green (Figure 7) (Patrignani and Ochsner 2015).

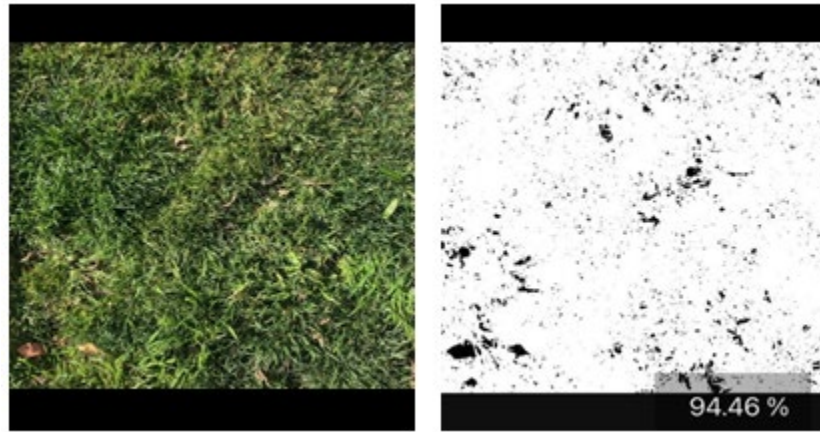


Figure 7. Side-by-side comparison of the difference between a digital color image of a lawn sample plot next to the same imaged processed using the Canopeo app.

To estimate the GPP of our vegetated samples at 100% FGCC, first we divided 100 by the observed FGCC of our sample using the following equation:

$$FGCC_{mult} = 100 \div FGCC_{obs} \quad (5)$$

$FGCC_{mult}$  was then used to estimate GPP at 100% FGCC. To do this we multiplied the observed GPP by  $FGCC_{mult}$  such that

$$GPP_{100} = FGCC_{mult} \times GPP_{obs} \quad (6)$$

The  $FGCC_{obs}$  of all the samples was measured on the fourth day of our study. We felt that a single  $FGCC_{obs}$ , per *L. longifolia*, was sufficient due to the plants little amount of growth within the study period. Both lawns were measured for  $FGCC_{obs}$  a second time two weeks after the first

measurement. Lawn A, due to having no supplemental watering, thus drying out, showed diminished  $FGCC_{obs}$  by 12.5%, while Lawn B showed an increase  $FGCC_{obs}$  by 1%. As a result,  $FGCC_{mult}$  was adjusted accordingly.

## 2.5 Data Processing

A linear regression analysis was used to calculate  $CO_2$  concentration change over time ( $\Delta C/\Delta t$ ) in all of our samples ( $n=260$ ). That change in  $CO_2$  concentration was determined from the slope of the linear relationship between the gas concentration and time in seconds. The variable ( $m$ ) in the linear equation  $y = mx+b$  refers to the slope of a line and is the same thing as  $\Delta C$  in (eq.1).

Our method for selecting the best series of data points to represent the most accurate  $CO_2$  flux was to use a 60 second “flux window”. The flux window began after the first 15 seconds the chamber was determined to be sealed. That initial 15 seconds was considered the settling period in which the chamber’s fan homogenized the air within the headspace following the disruption of placing and sealing the chamber.

## 2.6 Data Analysis

After each sample was processed, the resulting fluxes were inspected for anomalies within each linear regression. When applicable our 60-second flux window was adjusted, or data points removed, if periods of disturbance were detected within the chamber observation period, i.e., an unusual spike in  $CO_2$  concentration. However, even when the flux window was moved, or data points removed, to eliminate periods of disturbance the changes to fluxes were insignificant ( $< .01 \text{ mg } CO_2 \text{ m}^2$ ).

$R^2$  values from the linear regression analysis provided insight as to the accuracy of the flux measurements. Originally,  $R^2$  values greater than .75 were accepted as accurate. Below  $R^2 = .75$  data points were examined by cross-referencing our field notes for sudden changes to environmental conditions, like perturbations caused by wind gusts and unpredictable shading (passing clouds or the passing of large vehicles). In addition to analyses in our pilot study, we noticed a general trend when  $\text{CO}_2$  fluxes measured between  $R^2$  values were .40, or less  $\text{CO}_2$  fluxes measured between .01 and .04  $\text{mgCO}_2 \text{ m}^{-2} \text{ s}^{-1}$ . Therefore, outside of four individual plot measurements we used all measurement in our results. The four measurements which were removed represented  $\text{CO}_2$  fluxes inconsistent, in some cases opposite, of previous plot measurements for what was reasonable for that specific groundcover. For example, on DOY 74 two plots, L1 and B1, which consisted primarily of bark, registered as negative values (-1.69, -5.59 respectively), oddly suggesting strong GPP.

### 3 Results

#### 3.1 Soil characteristics and meteorological conditions throughout study

Soil temperatures over the study period changed based on variability associated with day-to-day differences in meteorological conditions rather than consistent change over time (Figure 8).

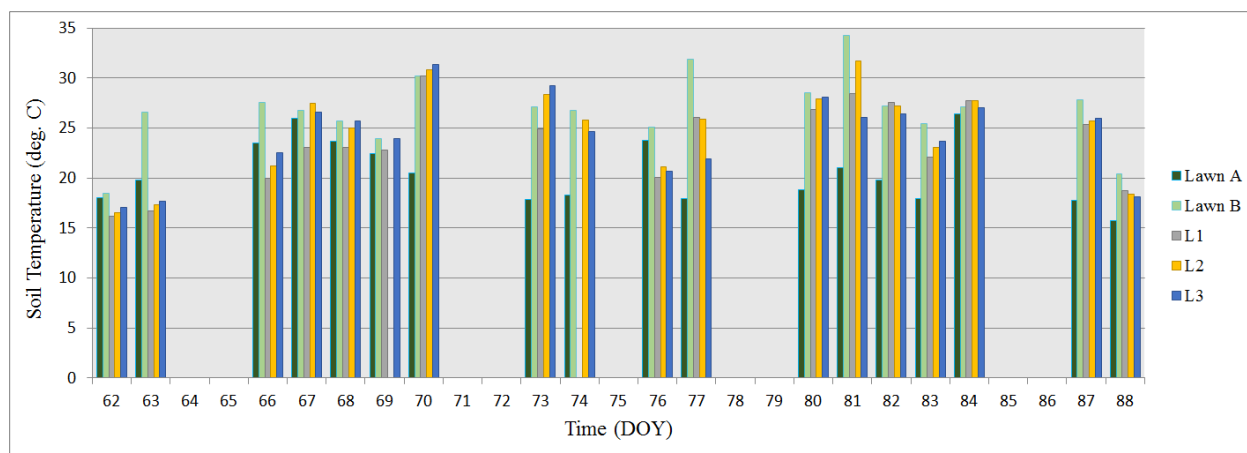


Figure 8. Plot average soil temperature per vegetated plot for each day we sampled across the entire study period.

An ANOVA test revealed there was enough evidence to reject the null hypothesis that the population means of  $T_{\text{soil}}$  were all equal (ANOVA,  $p=0.0002$ ,  $\alpha=.05$ ) (Appendix A). We found the greatest differences of  $T_{\text{soil}}$  when comparing Lawn A to Lawn B. Our daily spot measurement mean of Lawn A was 23 percent less than Lawn B. We ascertain that the difference in  $T_{\text{soil}}$  between lawns, in part, was due to the differences in time between when sampling occurred and

how long before the lawn was exposed to full sun. Lawn A was sampled shortly after the time when the plot first received full sun. On the contrary, Lawn B had received full sun for longer before sampling, thus having time to warm. Moreover, the local shading from buildings and trees, during times outside our sampling time, may have contributed to  $T_{\text{soil}}$  differences. Further statistical evidence suggests that the mean Lawn A  $T_{\text{soil}}$  mean was equal to L1, but not L2 or L3 (Figure 9). When comparing the average  $T_{\text{soil}}$  of the three *L. longifolia* an ANOVA test also revealed that there was no significant difference between any pair of means (ANOVA,  $p=0.68$ ,  $\alpha=.05$ ) (Appendix B).

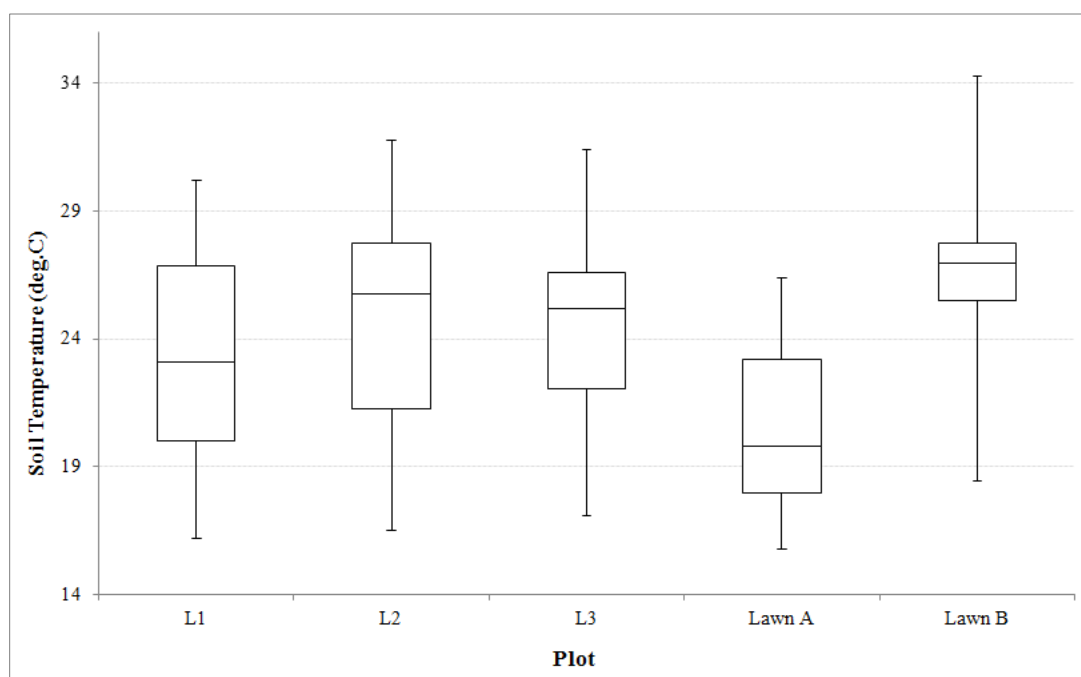


Figure 9. Box plot showing the variability in soil temperatures for vegetated plots over the entire study period

Similar to  $T_{\text{soil}}$ , soil moisture varied based on day-to-day differences in meteorological conditions, not a trend over the study period. All plots showed slight increases in soil moisture

after short periods of precipitation followed by moderated decreases to soil moisture, which then held steady until the next rain event. Periods in between precipitation were dominated by sunny and clear days, where we also recorded some of our largest PAR and  $T_{air}$  readings.

Lawn B measured consistently the highest in soil moisture throughout the entire study. Lawn B was also more than twice the VWC% of Lawn A, on 16 of 18 occasions (Figure 10). This was primarily due to Lawn A receiving no irrigation (except on DOY 84) and a low amount of precipitation (8 percent of normal since Jan.1, Oakland Int'l Airport NOAA weather station) (Figure 10). In comparison Lawn B was getting an indeterminable, yet consistent and ample amount of water via an underground source, likely Glen Echo creek.

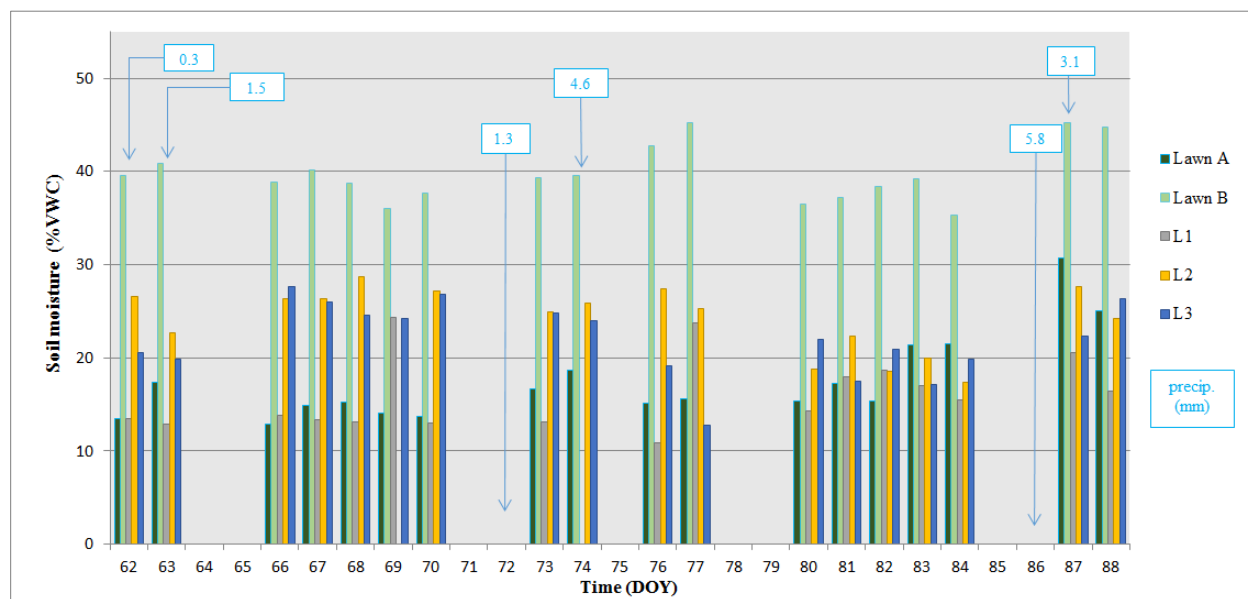


Figure 10. Plot average soil moisture observations for each vegetated plot with markers highlighting individual days of light precipitation recorded at the OAKLAND MUSEUM, CA US weather station (NOAA).

An ANOVA test revealed that, apart from pairs Lawn A-L1 and L2-L3, the population means of soil moisture for all other plots were statistically significantly different (ANOVA,  $p = 0$ )(Appendix C). The clearest differences were Lawn B measuring 147% larger than L1, and also 127% larger than Lawn A (Figure 11). *L. longifolia* samples showed less variability between one another. Plots L2 and L3 were statistically equal and larger than L1 by 51% and 37% respectively (Figure 11). The drier conditions found at site L1 are likely due the heterogeneity in underground drip lines. The fresh layer of Fir bark mulch, installed across all *L. longifolia* sample plots on DOY 75, did not impact soil moisture levels, however we did see more similarity in soil moisture in the three *L. longifolia* plots after day 75.

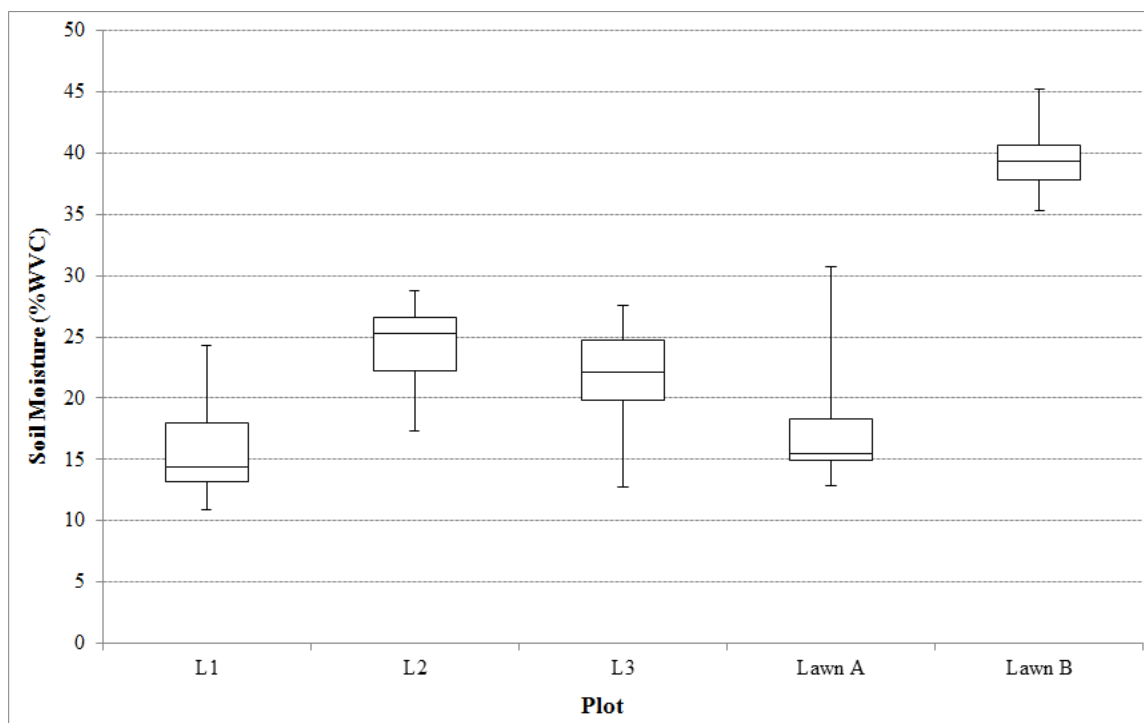


Figure 11. Box plot showing the variability in soil moisture across all vegetated plots for the entire study period.

The weather for a large majority of the days (during sampling times) was very similar: sunny and clear with very light to light winds. On those days PAR measurements averaged  $1329 \mu\text{mol m}^{-2} \text{s}^{-1}$ . The remaining few days were under decreasing cloudy conditions, resulting in an average PAR measurement of  $536 \mu\text{mol m}^{-2} \text{s}^{-1}$ . Light rain fell on six days, with a total of 16.6 mm over the study period, and a maximum of only 5.8 mm in one day (Figure 10).

### 3.2 Chamber fluxes

$\text{CO}_2$  flux measurements between all sample plots showed that lawn plots were significant sinks of  $\text{CO}_2$ . The average NEE between both lawns across the entire study period varied substantially (Welch's t-test,  $p=0.00007$ ,  $\alpha=.05$ ). While the maximum and minimum values of both lawns were very similar ( $-0.33 \pm 0.01$ ,  $-1.11 \pm 0.03$ ), Lawn B showed to be the stronger sink. At an average of  $-0.84 \text{ mgCO}_2 \text{ m}^{-2} \text{ s}^{-1}$ , Lawn B exceeded the NEE of Lawn A ( $-0.52 \text{ mgCO}_2 \text{ m}^{-2} \text{ s}^{-1}$ ) by 62 percent (Figure 12).

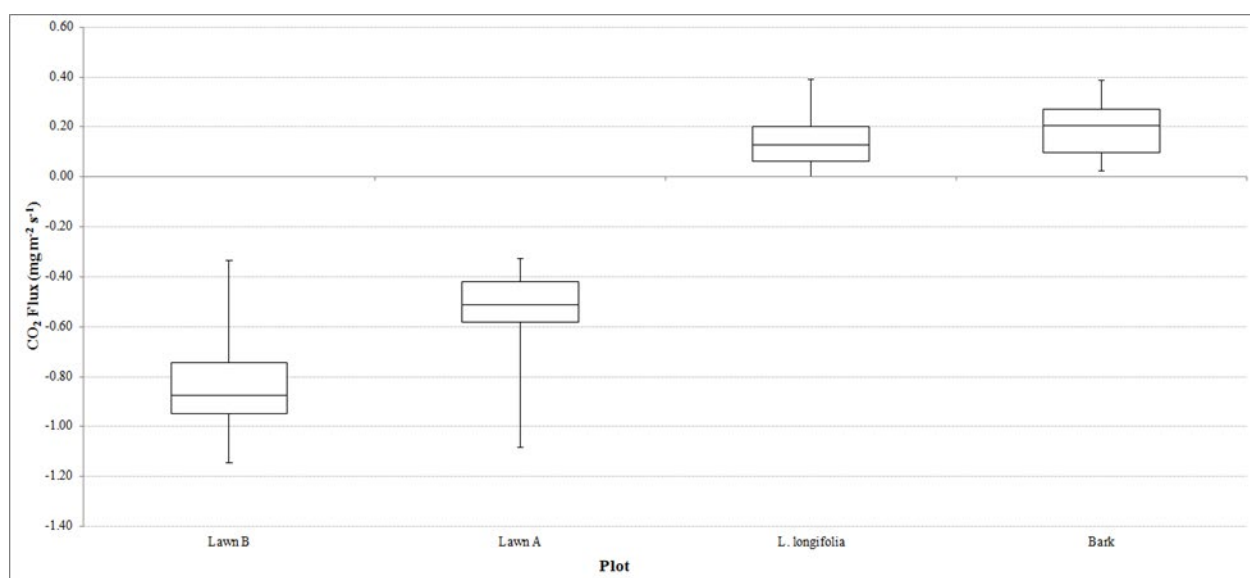


Figure 12. Box plot shows CO<sub>2</sub> fluxes of grouped *L. longifolia*, grouped bark plots and Lawns A and Lawn B, in ascending order based on each vegetated plot's flux mean

NEE in the *L. longifolia* plots were dominated by R<sub>cco</sub>, as expected and as a result were sources of CO<sub>2</sub> while closely resembling the NEE of our bark plots (Figure 12). We also expected to see NEE of *L. longifolia* plot correlate highly to soil moisture and T<sub>soil</sub>, however regression analyses of *L. longifolia* to all explanatory variables only showed plot L3 moderately significant to T<sub>soil</sub> (R<sup>2</sup> = 0.49) (Figure 13). Respiration was far greater than photosynthesis, as our *L. longifolia* plots consisted of >90% bark and our small plants made only up a small fraction of the chambers volume. There was enough evidence to accept the null hypothesis that the population means of all three *L. longifolia* plots were equal (ANOVA, p=0.32, α=.05) (Appendix D). Therefore, *L. longifolia* was considered as a group when compared to both lawn plots and bark (Figure 12). Similarly, all three bark plots had statically equal means of CO<sub>2</sub> fluxes as well (ANOVA, p=0.13, α=.05) (Appendix E).

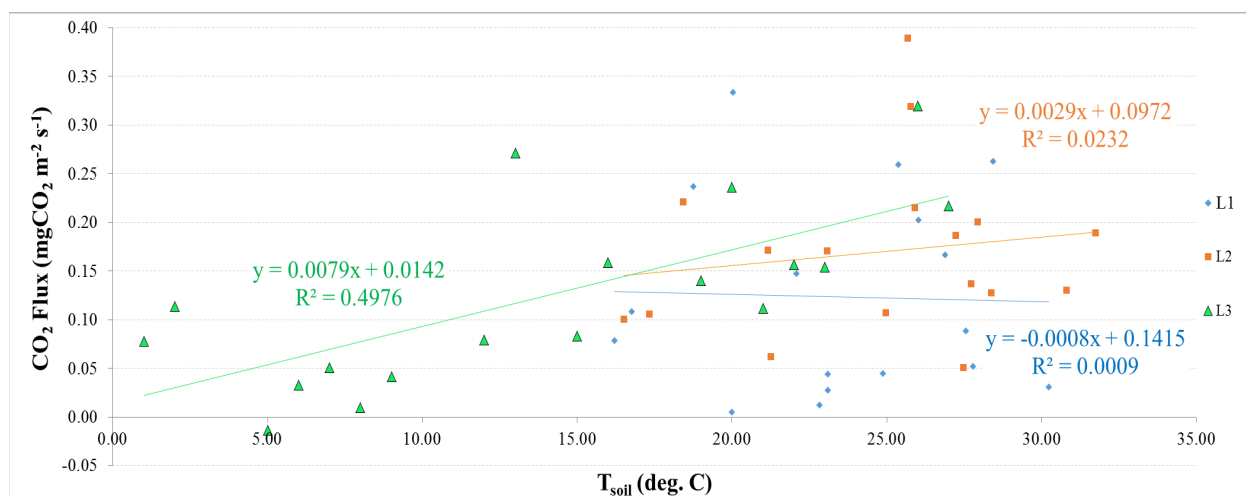


Figure 13. Relationship between CO<sub>2</sub> flux and T<sub>soil</sub> including linear regression analysis for the three *L. longifolia* plots.

R<sub>eco</sub> values were the direct calculations from our darkened chamber observations. Both Lawn plots emitted approximately twice as much CO<sub>2</sub> than *L. longifolia* or bark plots (Figure 15). Lawn B measured approximately 16 percent higher than Lawn A. Unexpectedly, only Lawn A showed the effects of soil moisture on R<sub>eco</sub>. Based on a linear regression analyses, Lawn A correlated positively with R<sub>eco</sub>, however only moderately (R<sup>2</sup> = 0.55) (Figure 14). No other significant trends were found between R<sub>eco</sub> and either air or soil temperature. However, both soil and climate conditions remained fairly consistent over the short observation period, where increases in soil moisture coincided with rain events and/or the one occasion when Lawn A was irrigated. So the effects of soil moisture and T<sub>soil</sub> would need to be tested with a longer dataset.

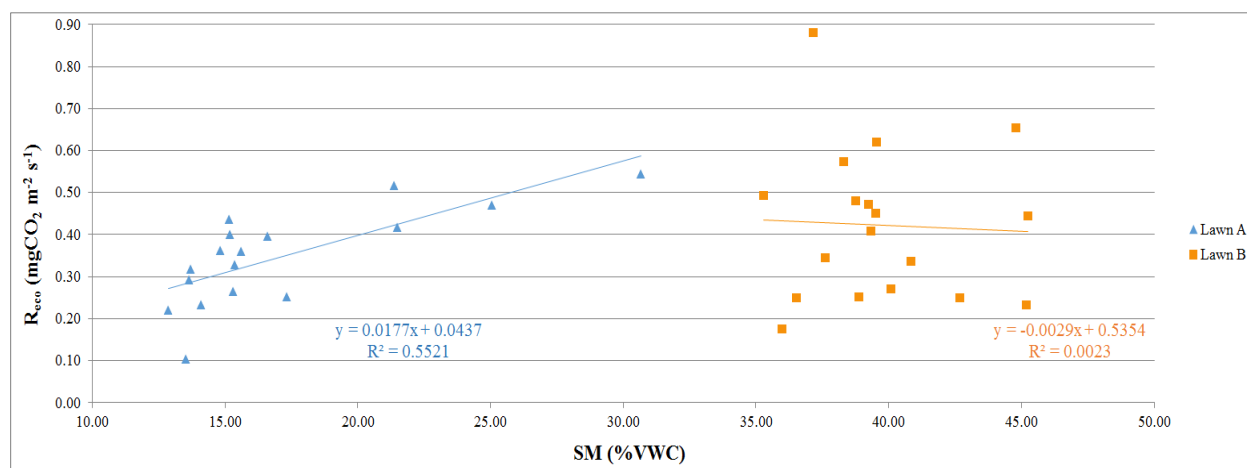


Figure 14. A linear regression shows the relationship between calculated plot average soil moisture and observed average R<sub>eco</sub> for both lawns over the entire study period.

Some of the averages between the  $R_{\text{eco}}$  from *L. longifolia* plots were not statistically equal (ANOVA,  $p=0.02$ ,  $\alpha=.05$ ) (Appendix E). Although, plots L1 and L3 were almost identical in terms of  $R_{\text{eco}}$ , L2 measured between 24-32% higher average  $R_{\text{eco}}$  than L1 and L3. This difference could be attributed to the higher soil moisture (8%) found for plot L2 than L1. The difference in soil moisture levels between L2 and L3 was negligible (1.9%) (Table 4).

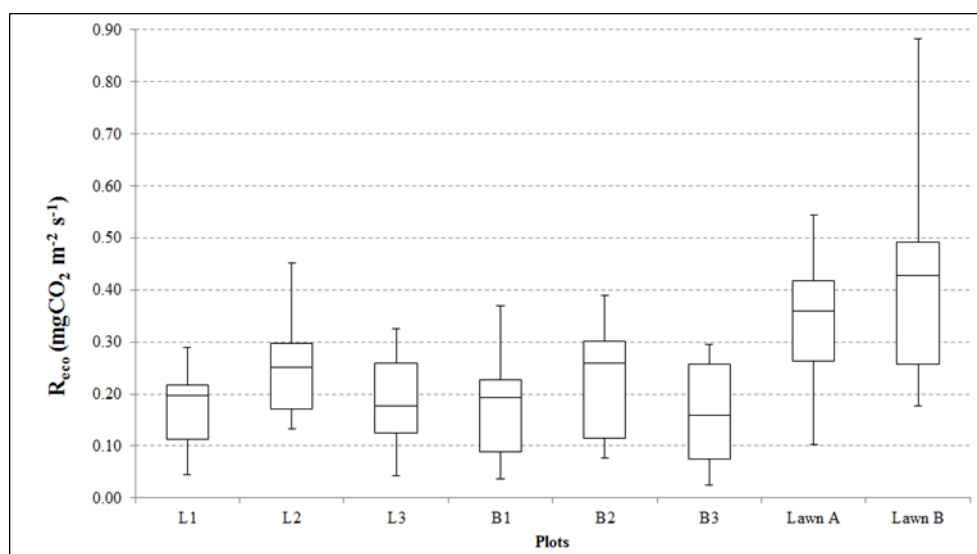


Figure 15. Box plot showing  $R_{\text{eco}}$  of all plots, in ascending order based on  $R_{\text{eco}}$  means across the entire study

Bark plots only produced  $R_{\text{eco}}$  since there were no photosynthesizing plants in the chamber, and because we attempted to mimic the plot without vegetation we expected to see slightly higher emissions than *L. longifolia* plots. When we compared *L. longifolia* to bark plots we saw an increase in mean  $R_{\text{eco}}$  by 35 percent.

We partitioned GPP by subtracting  $R_{\text{eco}}$  (which we obtained from our dark chamber measurements), from the NEE (which we calculated from transparent chamber measurements) (Equation 3). GPP far exceeded  $R_{\text{eco}}$  in both lawns, as each lawn plot had nearly complete

canopy cover compared to the individual juvenile *L. longifolia*, which had canopy covers of 4.3 and 7.8 percent. GPP values for each lawn provided enough evidence to assume them to have statistically different means (Welch's t-test,  $p=0.00001$ ,  $\alpha=.05$ ) (Table 4). The mean GPP of Lawn B was 62% greater than Lawn A (Table 4). However, Lawn A was the plot which showed a moderate correlation between GPP correlate to soil moisture ( $R^2 = 0.63$ ).

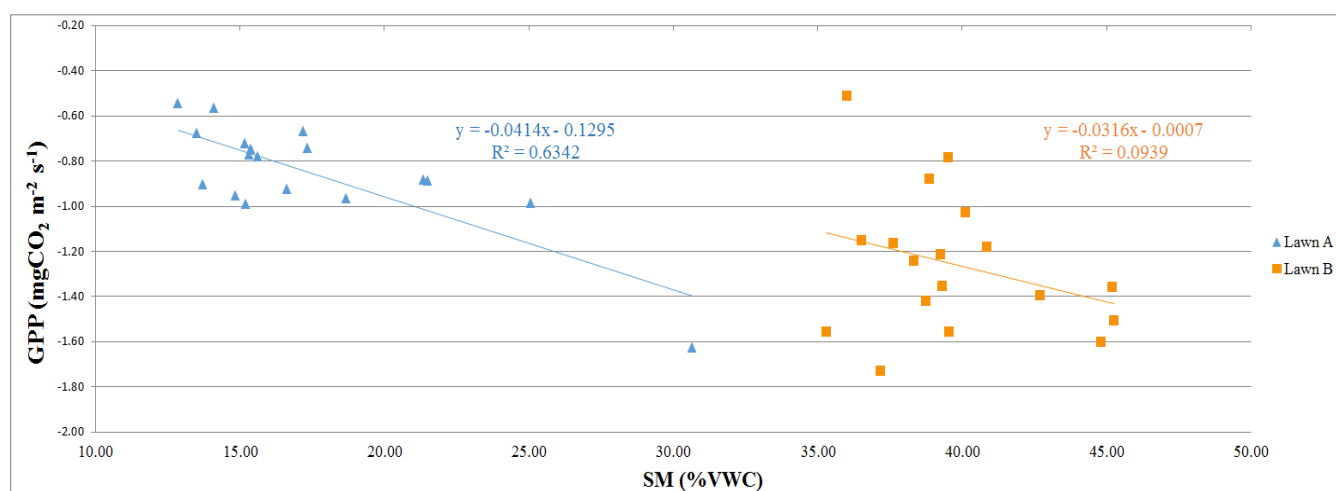


Figure 16. A linear regression shows the relationship between measured soil moisture and average GPP for both lawns over the entire study period.

Due to the similarity in size of the three *L. longifolias*, and thus their similarity in GPP, variation in average GPP amongst plots L1, L2, and L3 varied only slightly ( $\pm 0.03$  mgCO<sub>2</sub> m<sup>-2</sup> s<sup>-1</sup>). Moreover, based on a one-way ANOVA tests, there was enough evidence to accept the null hypothesis that the mean GPP of all *L. longifolia* were assumed to be equal ( $p=0.62$ ,  $\alpha=.05$ ) (Appendix F). However the difference in GPP means between the *L. longifolia* as a group and each lawn was large enough to be statistically significant.

		Lawn A	Lawn B	L1	L2	L3
NEE	Mean	-0.52	-0.84	0.12	0.16	0.12
	Max	-0.32	-0.33	0.33	0.39	0.32
	Min	-1.08	-1.14	0.01	0.05	-0.01
GPP	Mean	-0.85	-1.26	-0.07	-0.10	-0.07
	Max	-0.55	-0.51	0.00	0.02	0.00
	Min	-1.63	-1.73	-0.18	-0.26	-0.15
R <sub>eco</sub>	Mean	0.35	0.42	0.17	0.25	0.19
	Max	0.54	0.88	0.29	0.45	0.32
	Min	0.10	0.18	0.04	0.13	0.04

Table 4. Average NEE, GPP and R<sub>eco</sub> values, in units of mgCO<sub>2</sub> m<sup>-2</sup> s<sup>-1</sup>, for all vegetated plots over the entire study period

### 3.2 Estimated GPP associated with various Fractional Green Canopy Cover

To make estimations of how *L. longifolia* compared to Lawn in terms of GPP we scaled up all vegetated plots to GPP<sub>100</sub> using Equation 6. We recorded two FGCC observations at both lawns and one at each *L. longifolia* plot. On the 6<sup>th</sup> day of our study we recorded FGCC observations at all vegetated plots, and on 20<sup>th</sup> day we recorded FGCC observations from lawns exclusively. Due to the slow growth rate of *L. longifolia* a second FGCC observations was unwarranted. Results revealed that Lawn A had decreased in FGCC by 12.5 % and an increase of 1% in Lawn B. This was noticeably visible by patches of Lawn A turning brown, while Lawn B remained healthy. Environmental conditions, in combination with climate, in the time between FGCC<sub>obs</sub> measurements may have played a role in Lawn A's deterioration (T<sub>soil</sub> and T<sub>air</sub> showed slight increases, PAR a steep increase and soil moisture a moderate decrease), however Lawn A's stress was likely a result of the unseasonably long period of dry weather with little to no precipitation or irrigation. During the period between FGCC measurements DOY 67 and DOY 81 CO<sub>2</sub> fluxes generally increased (interpreted as a loss of strength in carbon sequestration),

however only slightly. Also, we saw one day where flux measurements spiked to 41 percent above the mean.

Table 5. FGCC observation measurements with GPP<sub>100</sub> estimations

	Lawn A		Lawn B		L1	L2	L3
	observation 1	observation 2	observation 1	observation 2	single observation		
<i>FGCC<sub>obs</sub></i> (%)	94.0	81.5	98.0	99.0	7.8	5.1	4.3
<i>FGCC<sub>mult</sub></i>	1.06	1.23	1.02	1.01	12.82	19.61	23.25
<i>GPP<sub>obs</sub></i>	-0.79 <sub>a</sub>	-0.97 <sub>b</sub>	-1.14 <sub>a</sub>	-1.47 <sub>b</sub>	-0.07 <sub>c</sub>	-0.09 <sub>c</sub>	-0.07 <sub>c</sub>
<i>GPP<sub>100</sub></i>	-0.84	-1.19	-1.16	-1.48	-0.90	-1.76	-1.63

\*All GPP units are in mgCO<sub>2</sub> m<sup>-2</sup> s<sup>-1</sup>  
<sup>a</sup> Average GPP based on study period *before* 2<sup>nd</sup> observation (DOY 62 thru DOY 80)  
<sup>b</sup> Average GPP based on study period *after* 2<sup>nd</sup> observation (DOY 80 thru DOY 88)  
<sup>c</sup> Average GPP based on complete study period

### 3.3 GPP of lawns and carbon sequestration potential of *L. longifolia*

Strictly based on GPP<sub>obs</sub>, the lawn plots sequestered an estimated ten times more mgCO<sub>2</sub> m<sup>-2</sup> s<sup>-1</sup> than *L. longifolias* plots during peak photosynthesis (Table 5). Also, when comparing the lawns to one another, taking in to account the differences in FGCC<sub>obs</sub>, Lawn B averaged approximately 47 percent more mgCO<sub>2</sub> m<sup>-2</sup> s<sup>-1</sup> than Lawn A.

GPP<sub>100</sub> offered us a way to scale up GPP estimates of the sparse *L. longifolias* canopy to the equivalent of full canopy cover of the lawns. At GPP<sub>100</sub>, all *L. longifolias*, hypothetically, exceeded the maximum GPP of either lawn. The largest difference between any two plots was L2 greater than Lawn B (2<sup>nd</sup> observation) by 110 percent (Figure 10).

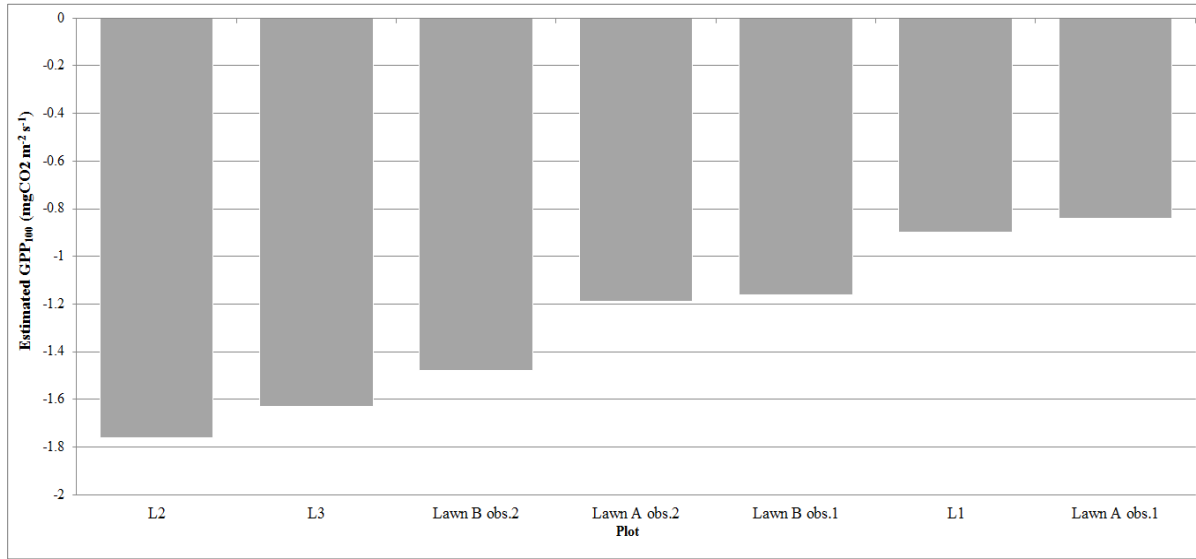


Figure 17. Estimated GPP<sub>100</sub> for all vegetated plots. Each lawn GPP<sub>100</sub> estimate shown further separated by observation periods 1 and 2 based on changes in FGCC. Observation 1 reflects observed GPP averages across the period from the start of study until our second FGCC observation (19 days). Observation 2 reflects the average GPP for the remainder of the study (8 days). Estimated GPP<sub>100</sub> from *L. longifolias* based on average observed GPP from entire study.

### 3.4 Autotrophic Respiration from *L. longifolia*

We set out to quantify  $R_{\text{auto}}$  of the *L. longifolias* to get an understanding of how much CO<sub>2</sub> emitted from *L. longifolias* directly contributed to  $R_{\text{eco}}$ . To calculate  $R_{\text{auto}}$  we subtracted  $R_{\text{het}}$  (bark only plot, which mimicked a *L. longifolia* plot without the plant in it) from  $R_{\text{eco}}$  (attained the dark chamber measurements). While we are confident that our dark chambers (with the *L. longifolia* inside) measured  $R_{\text{eco}}$  successfully, uncertainty arose when analyzing  $R_{\text{auto}}$ . We could only rely on the assumption that our transparent chamber, when moved to a plot as close to the *L. longifolia* sample without capturing the plant, would offer us sufficient  $R_{\text{het}}$  results. After calculating  $R_{\text{auto}}$ , using residuals from Equation 3, our results showed a mean  $R_{\text{auto}}$  of .01 mgCO<sub>2</sub> m<sup>-2</sup> s<sup>-1</sup> (Figure 11).



Figure 18. Autotrophic respiration based on calculated averages for all *L. longifolia* over entire study period

Due to *L. longifolia* only taking up a small portion of chamber footprint area (7.8% at most), based on  $\text{FGCC}_{\text{obs}}$ , it is likely that  $R_{\text{auto}}$  from *L. longifolia* was very small, potentially smaller than the differences in  $R_{\text{het}}$  across the study area. In addition, roughly a third of our calculations resulted in negative values suggesting that when moving the chamber (no more than 15 cm) resulted in recording  $R_{\text{het}}$  measurements larger than those previously recorded in the dark chamber before moving. Moreover, it is possible that weak amounts of photodegradation of the bark surface affected  $R_{\text{het}}$  differently under transparent than dark chamber methods.

### 3.5 Water Use

We calculated evapotranspiration (ET) averages for each vegetated plot based on the chamber measurements of H<sub>2</sub>O fluxes over the study period and compared these with average  $\text{GPP}_{\text{obs}}$  and soil moisture (SM) levels (Table 6). In doing so we were able to assess their relative

water usage in relation to carbon sequestration potential. The two lawns lost similar amounts of water to the atmosphere through ET, despite Lawn B having double the SM levels. The three *L. longifolia* plots were also similar to each other but lost less than half the water than the lawns. Lawn B had 77% higher soil moisture content than Lawn A, but sequestered only 26% more CO<sub>2</sub> (Table 6). Further, soil moisture results revealed that L1 had equal GPP<sub>obs</sub> to L3 while using 31% less water, suggesting the plant requires much less water than provided in L3. In addition, L1 used 40% less water than L2 while GPP<sub>obs</sub> only increased by 25%.

Table 6. Evapotranspiration, soil moisture and GPP<sub>obs</sub> for all vegetated plots. Evapotranspiration based on the averages of H<sub>2</sub>O flux observations over the entire study.

	Lawn A	Lawn B	L1	L2	L3
ET (gH <sub>2</sub> O m <sup>-2</sup> s <sup>-1</sup> )	0.054	0.055	0.025	0.025	0.024
SM (%VWC)	17.5	39.7	16.0	24.1	22.0
GPP <sub>obs</sub> (mgCO <sub>2</sub> m <sup>-2</sup> s <sup>-1</sup> )	-0.85	-1.26	-0.07	-0.09	-0.07

## 4 Discussion

The objective of this research, in part, was to provide information for urban land managers to inform decisions when choosing ground cover for climate change mitigation purposes. Our lawn samples measured as sinks during a short period of the day in early spring under weather conditions conducive for peak photosynthesis. However, our  $R_{eco}$  results show that the lawn plots emitted greater amounts of  $CO_2$  than any other sampled plots. Moreover, our  $R_{eco}$  results can be accepted as fluxes very similar to those that carry on throughout the night, when photosynthesis is zero.

By comparing lawn and *L. longifolia* plot  $R_{eco}$  averages we were afforded enough support to recommend planting *L. longifolia* versus lawn (in non-athletic field applications). In Figure 13 we show the mean  $R_{eco}$  across all vegetated plots. Using this data we calculated that *L. longifolia* plots emit between 35-50 percent less  $CO_2$  than lawn for roughly half of a 24-hour period, because  $R_{eco}$  can be interpreted as the amount of carbon which is emitted into the atmosphere during much of the night. More support for our recommendation came from estimates based on of the carbon sequestration capacity of *L. longifolia* when planted at high density.  $GPP_{100}$  values from Table 5 explain that *L. longifolia* closely compares to lawn in terms of carbon capture.

Here in California, where 95 percent of the state is classified as having “severe drought” conditions, the water use-to-carbon capture should be considered carefully in carbon-wise garden design (NOAA and NIDIS, n.d.). We were not able to compare irrigation regimes however our soil moisture results suggest that *L. longifolia* requires much less water to produce significant sequestration rates to lawns and lost less than half of the water of lawns to the atmosphere

through ET. Furthermore, we found that decreasing soil moisture for lawns can help lower  $R_{eco}$ . In our case, on average across the whole study, Lawn A soil moisture was half that of lawn B and emitted 10 percent less  $CO_2$ , at the cost of losing a small amount of aesthetic integrity (a 10 percent less green lawn).

Information on water needs per plant is well studied and readily available to consumers, also a common factor when making choice for designing a home garden. However, information on the carbon sequestration capacity of ornamental plants is scarce, uncommon outside of the scientific community, and therefore unavailable for consumers. With more information on the sequestration capacities per plant, from studies like ours, future commerce could include carbon sequestration-to-water use calculations on labels and in advertising, thus offering consumers climate-smart options and raise awareness. Further, when more information is known about the carbon sequestration capacities of more common garden plants the idea of incentivizing (e.g. lawn removal programs or carbon markets) changing gardens to promote carbon sequestration becomes realistic.

## 5 Conclusion

Our study presented the variability in CO<sub>2</sub> fluxes from two lawns, three *L. longifolia* and three bark mulched plots across two residential gardens. Using transparent and darkened versions of the closed chamber method we calculated NEE, R<sub>eco</sub>, GPP. In addition, both R<sub>auto</sub> and R<sub>het</sub> emissions associated *L. longifolia* were estimated. In doing so, our study contributed to the development of climate mitigation research at the micro-scale in urban environments, which is understudied and where much is unknown.

The chamber method proved to be a valuable tool for tackling the problem of heterogeneity in land cover types so often found in urban gardens. As a result we saw large differences in average flux magnitudes. At an average of -0.88 mgCO<sub>2</sub> m<sup>-2</sup> s<sup>-1</sup> Lawn B measured as the strongest sink, and was a stronger sink than Lawn A by 62 percent. The bark plots on average emitted 0.20 mgCO<sub>2</sub> m<sup>-2</sup> s<sup>-1</sup> and measured as the largest source over the course of our study. We identified the potential for *L. longifolia* to sequester similar amounts of CO<sub>2</sub> as a traditional lawn if planted at a high density, while using less water than traditional lawn in the process.

Future studies will need to include similar experimental designs but for longer study periods. Studies of a year, or more, have the potential to compare CO<sub>2</sub> fluxes over an entire growing season, including different phases of plant growth. In addition, longer studies allow for the investigation of how GHG fluxes vary in relation to environmental drivers, especially soil temperature, soil moisture and cloudiness.

Our study only captured a small sample of common ground covers. The expansion to other garden types, like residential fruit and vegetable gardens, water gardens or container gardening will aid in better understanding GHG fluxes in the urban setting. Moreover, the inclusion of trees will make urban study more comprehensive. However this would involve larger chambers or alternative methods such as dendrometer bands and sap flow sensors. Also sampling mature plants will eliminate the difficulties in comparing plants based on age or density.

The inclusion of methane fluxes to micro-scale urban study will afford researchers data on how a GHG approximately 25 times more potent than CO<sub>2</sub> to global warming functions within urban wetlands. Also, measuring nitrous oxide fluxes will allow for the better understanding of the trade-offs between using nitrogen-based garden amendments for plant health versus contributing another powerful GHG to the atmosphere. Furthermore, by including more explanatory variables, like soil pH, soil bulk density, VPD and the measuring of carbon to nitrogen ratios, will help rank drivers to better assist in choice-making for urban land managers. Also, by sampling the same plots multiple times a day would allow for the calculation of rates where GPP drops off further determining when lawns turn from sinks to sources. Lastly, the carbon costs of installing and maintaining home gardens should also be considered when trying to gather an entire perspective of the net ecosystem exchange of CO<sub>2</sub> in urban gardens.

Micro-scale studies like ours are largely carried out by universities and/or the private sector. Optimistically, governmental agencies will provide support in the near future in an effort to bolster and speed up our understanding of GHG fluxes in urban areas.

## 6 References

- Andersen, J. K., A. Boldrin, T. H. Christensen, and C. Scheutz. 2010. "Greenhouse Gas Emissions from Home Composting of Organic Household Waste." *Waste Management* 30 (12): 2475–82. <https://doi.org/10.1016/j.wasman.2010.07.004>.
- Beesley, Luke. 2012. "Carbon Storage and Fluxes in Existing and Newly Created Urban Soils." *Journal of Environmental Management* 104: 158–65. <https://doi.org/10.1016/j.jenvman.2012.03.024>.
- Berry, Z. Carter, and Gregory R. Goldsmith. 2020. "Diffuse Light and Wetting Differentially Affect Tropical Tree Leaf Photosynthesis." *New Phytologist* 225 (1): 143–53. <https://doi.org/10.1111/nph.16121>.
- Bezyk, Yaroslav, Maxim Dorodnikov, Agnieszka Grzelka, and Alicja Nych. 2018. "Characteristics of Temporal Variability of Urban Ecosystem-Atmosphere CO<sub>2</sub>, CH<sub>4</sub>, and N<sub>2</sub>O Fluxes." *E3S Web of Conferences* 44. <https://doi.org/10.1051/e3sconf/20184400013>.
- Byrne, Loren B., Mary Ann Bruns, and Ke Chung Kim. 2008. "Ecosystem Properties of Urban Land Covers at the Aboveground-Belowground Interface." *Ecosystems* 11 (7): 1065–77. <https://doi.org/10.1007/s10021-008-9179-3>.
- Chadha, Aakansha, Singarayer K. Florentine, Bhagirath S. Chauhan, Benjamin Long, and Mithila Jayasundera. 2018. "Influence of Soil Moisture Regimes on Growth, Photosynthetic Capacity, Leaf Biochemistry and Reproductive Capabilities of the Invasive Agronomic Weed; *Lactuca Serriola*." *PLoS ONE* 14 (6): 1–17. <https://doi.org/10.1371/journal.pone.0218191>.
- Chun, J. A., K. Szlavecz, M. Bernard, D. Ferrer, J. Hom, and N. Saliendra. 2014. "Estimation of

- CO<sub>2</sub> Effluxes from Suburban Forest Floor and Grass Using a Process-Based Model.”  
*Atmospheric Environment* 97: 346–52. <https://doi.org/10.1016/j.atmosenv.2014.08.044>.
- Churkina, Galina. 2016. “The Role of Urbanization in the Global Carbon Cycle.” *Frontiers in Ecology and Evolution* 0 (JAN): 144. <https://doi.org/10.3389/FEVO.2015.00144>.
- Dai, Aiguo. 2013. “Erratum: Increasing Drought under Global Warming in Observations and Models.” *Nature Climate Change* 3 (2): 171. <https://doi.org/10.1038/nclimate1811>.
- Dyukarev, Egor A. 2017. “Partitioning of Net Ecosystem Exchange Using Chamber Measurements Data from Bare Soil and Vegetated Sites.” *Agricultural and Forest Meteorology* 239: 236–48. <https://doi.org/10.1016/j.agrformet.2017.03.011>.
- Goenster, Sven, Martin Wiehle, Martina Predotova, Jens Gebauer, Abdalla Mohamed Ali, and Andreas Buerkert. 2015. “Gaseous Emissions and Soil Fertility of Homegardens in the Nuba Mountains, Sudan.” *Journal of Plant Nutrition and Soil Science* 178 (3): 413–24. <https://doi.org/10.1002/jpln.201400292>.
- Grossiord, Charlotte, Thomas N. Buckley, Lucas A. Cernusak, Kimberly A. Novick, Benjamin Poulter, Rolf T.W. Siegwolf, John S. Sperry, and Nate G. McDowell. 2020. “Plant Responses to Rising Vapor Pressure Deficit.” *New Phytologist* 226 (6): 1550–66. <https://doi.org/10.1111/nph.16485>.
- Haciogullari, Nadiriye. 2012. “Effects Of Different Biobased Mulch Types On Photosynthesis, Transpiration And Stomatal Conductance Of Quercus Nuttallii Saplings.” Graduate School Southern University and A&M College.
- Hill, Andrew C., Josep Barba, John Hom, and Rodrigo Vargas. 2021. “Patterns and Drivers of Multi-Annual CO<sub>2</sub> Emissions within a Temperate Suburban Neighborhood.”

- Biogeochemistry* 152 (1): 35–50. <https://doi.org/10.1007/s10533-020-00731-1>.
- IPCC. 2014. “IPCC, 2014: Climate Change 2014: Synthesis Report. Contribution of Working Groups I, II and III to the Fifth Assessment Report of the Intergovernmental Panel on Climate Change [Core Writing Team, IPCC, Geneva, Switzerland, 151 Pp.” Geneva.
- IPCC. 2018. “IPCC Special Report ‘Global Warming of 1.5°C’ Summary for Teachers.” [https://www.ipcc.ch/site/assets/uploads/sites/2/2018/12/ST1.5\\_OCE\\_LR.pdf](https://www.ipcc.ch/site/assets/uploads/sites/2/2018/12/ST1.5_OCE_LR.pdf).
- Ito, Akihiko. 2020. “Constraining Size-Dependence of Vegetation Respiration Rates.” *Scientific Reports*, 1–8. <https://doi.org/10.1038/s41598-020-61239-0>.
- J . S . Singh and S . R . Gupta. 2016. “Plant Decomposition and Soil Respiration in Terrestrial Ecosystems Author ( s ): Published by : Springer on Behalf of New York Botanical Garden Press Stable URL : <Http://Www.Jstor.Org/Stable/4353928> Accessed : 15-03-2016 06.” *Botanical Review* 43 (4): 449–528.
- Kaye, Jason P., R. L. McCulley, and I. C. Burke. 2005. “Carbon Fluxes, Nitrogen Cycling, and Soil Microbial Communities in Adjacent Urban, Native and Agricultural Ecosystems.” *Global Change Biology* 11 (4): 575–87. <https://doi.org/10.1111/j.1365-2486.2005.00921.x>.
- Krekel, Christian, Jens Kolbe, and Henry Wüstemann. 2016. “The Greener, the Happier? The Effect of Urban Land Use on Residential Well-Being.” *Ecological Economics* 121: 117–27. <https://doi.org/10.1016/j.ecolecon.2015.11.005>.
- Legiandenyi, Thomas Nyatta. 2010. “Impact Of Different Biobased Mulches On The Urban Soil Co 2 Flux In Southern Louisiana.” Graduate School Southern University and A & M College.
- Livesley, Stephen J., Ben J. Dougherty, Alison J. Smith, Damian Navaud, Luke J. Wylie, and

- Stefan K. Arndt. 2010. "Soil-Atmosphere Exchange of Carbon Dioxide, Methane and Nitrous Oxide in Urban Garden Systems: Impact of Irrigation, Fertiliser and Mulch." *Urban Ecosystems* 13 (3): 273–93. <https://doi.org/10.1007/s11252-009-0119-6>.
- Memoli, V., A. De Marco, D. Baldantoni, Flavia De Nicola, and G. Maisto. 2017. "Short- and Long-Term Effects of a Single Application of Two Organic Amendments." *Ecosphere* 8 (11). <https://doi.org/10.1002/ecs2.2009>.
- Monteiro, José A. 2017. "Ecosystem Services from Turfgrass Landscapes." *Urban Forestry and Urban Greening* 26 (April): 151–57. <https://doi.org/10.1016/j.ufug.2017.04.001>.
- NOAA. n.d. "National Weather Service." <https://www.weather.gov/wrh/Climate?wfo=mtr>.
- NOAA, and NIDIS. n.d. "Drought.Gov." <https://www.drought.gov/states/california>.
- Oliphant, A. J., D. Dragoni, B. Deng, C. S.B. Grimmond, H. P. Schmid, and S. L. Scott. 2011. "The Role of Sky Conditions on Gross Primary Production in a Mixed Deciduous Forest." *Agricultural and Forest Meteorology* 151 (7): 781–91. <https://doi.org/10.1016/j.agrformet.2011.01.005>.
- Patrignani, Andres, and Tyson E. Ochsner. 2015. "Canopeo: A Powerful New Tool for Measuring Fractional Green Canopy Cover." *Agronomy Journal* 107 (6): 2312–20. <https://doi.org/10.2134/agronj15.0150>.
- Pramanik, P., K. K. Bandyopadhyay, Debarati Bhaduri, Ranjan Bhattacharyya, and P. Aggarwal. 2015. "Effect of Mulch on Soil Thermal Regimes - A Review." *International Journal of Agriculture, Environment and Biotechnology* 8 (3): 645. <https://doi.org/10.5958/2230-732x.2015.00072.8>.
- Raich, James W., and Aydin Tufekcioglu. 2000. "Vegetation and Soil Respiration: Correlations

- and Controls.” *Biogeochemistry* 48 (1): 71–90. <https://doi.org/10.1023/A:1006112000616>.
- Ros, M., S. Klammer, B. Knapp, K. Aichberger, and H. Insam. 2006. “Long-Term Effects of Compost Amendment of Soil on Functional and Structural Diversity and Microbial Activity.” *Soil Use and Management* 22 (2): 209–18. <https://doi.org/10.1111/j.1475-2743.2006.00027.x>.
- Ryan, Michael G., and Beverly E. Law. 2005. “Interpreting, Measuring, and Modeling Soil Respiration.” *Biogeochemistry* 73 (1): 3–27. <https://doi.org/10.1007/s10533-004-5167-7>.
- Saidani, Michael, and Harrison Kim. 2021. “Quantification of the Environmental and Economic Benefits of the Electrification of Lawn Mowers on the US Residential Market.” *International Journal of Life Cycle Assessment*, 1267–84. <https://doi.org/10.1007/s11367-021-01917-x>.
- San Joaquin Valley Air Pollution Control District. 2013. “Greenwaste Compost Site Emissions Reductions from Solar-Powered Aeration and Biofilter Layer Report from the Contract Team.”
- Saviozzi, A., R. Cardelli, P. N’kou, R. Levi-Minzi, and R. Riffaldi. 2006. “Soil Biological Activity as Influenced by Green Waste Compost and Cattle Manure.” *Compost Science and Utilization* 14 (1): 54–58. <https://doi.org/10.1080/1065657X.2006.10702263>.
- Shchepeleva, A. S., V. I. Vasenev, I. M. Mazirov, I. I. Vasenev, I. S. Prokhorov, and D. D. Gosse. 2017. “Changes of Soil Organic Carbon Stocks and CO<sub>2</sub> Emissions at the Early Stages of Urban Turf Grasses’ Development.” *Urban Ecosystems* 20 (2): 309–21. <https://doi.org/10.1007/s11252-016-0594-5>.
- The World Bank. 2021. “Urban Development.” 2021.

<https://www.worldbank.org/en/topic/urbandevelopment/overview#1>.

Townsend-Small, Amy, and Claudia I. Czimczik. 2010a. “Carbon Sequestration and Greenhouse Gas Emissions in Urban Turf.” *Geophysical Research Letters* 37 (2): 1–6.

<https://doi.org/10.1029/2009GL041675>.

Townsend-Small, Amy, and Claudia I. Czimczik. 2010b. “Correction to ‘Carbon Sequestration and Greenhouse Gas Emissions in Urban Turf.’” *Geophysical Research Letters* 37 (6): n/a-n/a. <https://doi.org/10.1029/2010gl042735>.

USDA-NRCS. n.d. “Web Soil Survey.”

<https://websoilsurvey.sc.egov.usda.gov/App/WebSoilSurvey.aspx>.

Vasenev, V., M. Varentsov, P. Konstantinov, O. Romzaykina, I. Kanareykina, Y. Dvornikov, and V. Manukyan. 2021. “Projecting Urban Heat Island Effect on the Spatial-Temporal Variation of Microbial Respiration in Urban Soils of Moscow Megalopolis.” *Science of the Total Environment* 786: 147457. <https://doi.org/10.1016/j.scitotenv.2021.147457>.

Velasco, E., M. Roth, S. H. Tan, M. Quak, S. D.A. Nabarro, and L. Norford. 2013. “The Role of Vegetation in the CO<sub>2</sub> Flux from a Tropical Urban Neighbourhood.” *Atmospheric Chemistry and Physics* 13 (20): 10185–202. <https://doi.org/10.5194/acp-13-10185-2013>.

Velasco, Erik, Elvagrís Segovia, Amy M.F. Choong, Benjamin K.Y. Lim, and Rodrigo Vargas.

2021. “Carbon Dioxide Dynamics in a Residential Lawn of a Tropical City.” *Journal of Environmental Management* 280 (November 2020): 111752.

<https://doi.org/10.1016/j.jenvman.2020.111752>.

Vergara, Sintana E, and Whendee L Silver. 2019. “Greenhouse Gas Emissions from Windrow Composting of Organic Wastes: Patterns and Emissions Factors.” *Environmental Research*

*Letters* 14 (12): 124027. <https://doi.org/10.1088/1748-9326/ab5262>.

Weissert, L F, J A Salmond, and L Schwendenmann. 2014. “Urban Climate” 8: 100–125.

<https://doi.org/10.1016/j.uclim.2014.01.002>.

Wherley, Benjamin G, and Thomas R Sinclair. 2009. “Differential Sensitivity of C 3 and C 4

Turfgrass Species to Increasing Atmospheric Vapor Pressure Deficit” 67: 372–76.

<https://doi.org/10.1016/j.envexpbot.2009.07.003>.

White, Mathew P., Ian Alcock, Benedict W. Wheeler, and Michael H. Depledge. 2013. “Would

You Be Happier Living in a Greener Urban Area? A Fixed-Effects Analysis of Panel Data.”

*Psychological Science* 24 (6): 920–28. <https://doi.org/10.1177/0956797612464659>.

Wurm, Ted. 1990. “Historic Piedmont Avenue.” *Oakland Heritage Alliance*, 1990.

<https://www.panil.org/wp-content/uploads/2021/02/OHA-Avenue-history.pdf>.

Appendix A. One-way ANOVA test and Tukey HSD test results for  $T_{soil}$  on all plots

## ANOVA

Source	D F	Sum of Square	Mean Square	F Statistic	P-value
Groups (between groups)	4	366.4396	91.6099	6.0495	0.0002539
Error (within groups)	83	1256.9041	15.1434		
Total	87	1623.3436	18.6591		

## Tukey HSD

Pair	Difference	SE	Q	Lower CI	Upper CI	Critical Mean	p-value
Lawn A-Lawn B	6.1983	0.9172	6.7577	2.581	9.8156	3.6173	0.00007264
Lawn A – L1	3.0094	0.9306	3.2338	-0.6607	6.6795	3.6701	0.1596
Lawn A – L2	4.2676	0.9306	4.5858	0.5975	7.9378	3.6701	0.01434
Lawn A – L3	3.7461	0.9172	4.0842	0.1288	7.3634	3.6173	0.03863
Lawn B – L1	3.1889	0.9306	3.4267	-0.4812	6.859	3.6701	0.1194
Lawn B – L2	1.9307	0.9306	2.0746	-1.7394	5.6008	3.6701	0.5866
Lawn B – L3	2.4522	0.9172	2.6735	-1.1651	6.0695	3.6173	0.3305
L1- L2	1.2582	0.9438	1.3331	-2.4639	4.9804	3.7222	0.8793
L1 - L3	0.7367	0.9306	0.7916	-2.9334	4.4068	3.6701	0.9804
L2 – L3	0.5215	0.9306	0.5604	-3.1486	4.1917	3.6701	0.9947

Appendix B. One-way ANOVA test and Tukey HSD test results for  $T_{\text{soil}}$  on all *L. longifolia* plots

ANOVA

Source	DF	Sum of Square	Mean Square	F Statistic	P-value
<b>Groups</b> (between groups)	2	13.593	6.7965	0.3821	0.6845
<b>Error</b> (within groups)	49	871.6468	17.7887		
<b>Total</b>	51	885.2398	17.3576		

Tukey HSD

Pair	Difference	SE	Q	Lower CI	Upper CI	Critical Mean	p-value
L1-x2	1.2582	1.0229	1.23	-2.2382	4.7547	3.4964	0.6617
x1-x3	0.7367	1.0086	0.7304	-2.7108	4.1842	3.4475	0.8637
x2-x3	0.5215	1.0086	0.5171	-2.926	3.9691	3.4475	0.9291

## Appendix C. One-way ANOVA test and Tukey HSD test results for soil moisture on all plots

## ANOVA

Source	DF	Sum of Square	Mean Square	F Statistic	P-value
<b>Groups</b> (between groups)	4	6374.9048	1593.7262	108.0007	0
<b>Error</b> (within groups)	83	1224.8006	14.7566		
<b>Total</b>	87	7599.7054	87.3529		

## Tukey HSD

Pair	Difference	SE	Q	Lower CI	Upper CI	Critical Mean	p-value
Lawn A-Lawn B	22.2694	0.9054	24.5953	18.6986	25.8403	3.5708	1.555e-10
Lawn A – L1	1.4276	0.9187	1.554	-2.1954	5.0505	3.6229	0.8067
Lawn A – L2	6.6736	0.9187	7.2645	3.0507	10.2965	3.6229	0.00001773
Lawn A – L3	4.5372	0.9054	5.0111	0.9664	8.108	3.5708	0.005731
Lawn B – L1	23.697	0.9187	25.7954	20.0741	27.32	3.6229	1.555e-10
Lawn B – L2	15.5958	0.9187	16.9768	11.9729	19.2188	3.6229	1.555e-10
Lawn B – L3	17.7322	0.9054	19.5842	14.1614	21.303	3.5708	1.555e-10
L1- L2	8.1012	0.9317	8.6952	4.4268	11.7755	3.6743	2.596e-7
L1 - L3	5.9648	0.9187	6.493	2.3419	9.5877	3.6229	0.0001484
L2 – L3	2.1364	0.9187	2.3255	-1.4866	5.7593	3.6229	0.4738

Appendix D. One-way ANOVA test and Tukey HSD test results for NEE on *L. longifolia* plots

ANOVA

Source	DF	Sum of Square	Mean Square	F Statistic	P-value
<b>Groups</b> (between groups)	2	0.02054	0.01027	1.1724	0.318
<b>Error</b> (within groups)	50	0.4379	0.008758		
<b>Total</b>	52	0.4584	0.008816		

Tukey HSD

Pair	Difference	SE	Q	Lower CI	Upper CI	Critical Mean	p-value
L1-L2	0.04203	0.02238	1.8779	-0.03442	0.1185	0.07645	0.3866
L1-L3	0.000915	0.02238	0.04089	-0.07553	0.07736	0.07645	0.9995
L2-L3	0.04111	0.02206	1.8639	-0.03423	0.1165	0.07535	0.392

## Appendix E. One-way ANOVA test and Tukey HSD test results for NEE on bark plots

## ANOVA

Source	DF	Sum of Square	Mean Square	F Statistic	P-value
<b>Groups</b> (between groups)	2	0.04259	0.02129	2.1045	0.1328
<b>Error</b> (within groups)	49	0.4958	0.01012		
<b>Total</b>	51	0.5384	0.01056		

## Tukey HSD

Pair	Difference	SE	Q	Lower CI	Upper CI	Critical Mean	p-value
B1-B2	0.05667	0.02406	2.3557	-0.02555	0.1389	0.08222	0.2286
B1-B3	0.006471	0.0244	0.2652	-0.07692	0.08986	0.08339	0.9808
B2-B3	0.06314	0.02406	2.6247	-0.01908	0.1454	0.08222	0.1625

Appendix F. One-way ANOVA test and Tukey HSD test results for  $R_{eco}$  on *L. longifolia* plots

## ANOVA

Source	DF	Sum of Square	Mean Square	F Statistic	P-value
<b>Groups</b> (between groups)	2	0.0558	0.0279	4.0068	0.0242
<b>Error</b> (within groups)	51	0.3551	0.006964		
<b>Total</b>	53	0.4109	0.007754		

## Tukey HSD

Pair	Difference	SE	Q	Lower CI	Upper CI	Critical Mean	p-value
L1 Dark-L2 Dark	0.07444	0.01967	3.7848	0.007297	0.1416	0.06715	0.02655
L1 Dark-L3 Dark	0.015	0.01967	0.7626	-0.05215	0.08215	0.06715	0.8524
L2 Dark-L3 Dark	0.05944	0.01967	3.0222	-0.007703	0.1266	0.06715	0.09242

Appendix G. One-way ANOVA test and Tukey HSD test results for GPP on *L. longifolia* plots

## ANOVA

Source	DF	Sum of Square	Mean Square	F Statistic	P-value
Groups (between groups)	2	0.003529	0.001765	0.484	0.6195
Error (within groups)	45	0.1641	0.003646		
Total	47	0.1676	0.003566		

## Tukey HSD

Pair	Difference	SE	Q	Lower CI	Upper CI	Critical Mean	p-value
L1-L2	0.01361	0.01541	0.8835	-0.0392	0.06643	0.05281	0.8074
L1-L3	0.006386	0.01541	0.4145	-0.04643	0.0592	0.05281	0.9538
L2-L3	0.02	0.01464	1.3657	-0.03019	0.07019	0.05019	0.6021